1995

Carbonate deposition, Pyramid Lake subbasin, Nevada: 2. Lake levels and polar jet stream positions reconstructed from radiocarbon ages and elevations of carbonates (tufas) deposited in the Lahontan basin

Larry Benson
U.S. Geological Survey, great.basin666@gmail.com

Michaele Kashgarian
Lawrence Livermore National Laboratory

Meyer Rubin
U.S. Geological Survey

ELSEVIER

Palaeogeography, Palaeoclimatology, Palaeoecology 117 (1995) 1–30

PALAEO GEOGRAPHY CLIMATOLOGY ECOLOGY

Carbonate deposition, Pyramid Lake subbasin, Nevada: 2. Lake levels and polar jet stream positions reconstructed from radiocarbon ages and elevations of carbonates (tufas) deposited in the Lahontan basin

Larry Benson [a], Michaele Kashgarian [b], Meyer Rubin [c]

[a] *U.S. Geological Survey, 3215 Marine St., Boulder, CO 80303, USA*

[b] *Center for Accelerator Mass Spectrometry, Lawrence Livermore National Laboratory, P.O. Box 808, L-397, Livermore, CA 94550, USA*

[c] *U.S. Geological Survey, M.S. 971, 12201 Sunrise Valley Drive, Reston, VI 22092, USA*

Received 2 August 1994; revised and accepted 11 October 1994

Abstract

Most of the tufas in the Pyramid Lake subbasin were deposited within the last 35,000 yr, including most of the mound tufas that border the existing lake. Many of the older tufas (>21,000 yr B.P.) contained in the mounds were formed in association with ground-water discharge. The radiocarbon (^{14}C) ages of the older tufas represent maximum estimates of the time of their formation. Lake Lahontan experienced large and abrupt rises in level at ~22,000, 15,000, and 11,000 yr B.P. and three abrupt recessions in level at ~16,000, 13,600, and 10,000 yr B.P. The lake-level rises that were initiated at ~23,500 and 15,500 yr B.P. are believed to indicate the passage of the polar jet stream over the Lahontan basin. During expansion of the Laurentide Ice Sheet, the jet stream moved south across the basin, and during the contraction of the Ice Sheet, the jet stream moved north across the basin.

The bulk of the carbonate contained in the mound tufas was deposited during the last major lake cycle (~23,500–12,000 yr B.P.), indicating that ground- and surface-water discharges increased at ~23,500 and decreased at ~12,000 yr B.P. A lake-level oscillation that occurred between 11,000 and 10,000 yr B.P. is represented by a 2-cm thick layer of dense laminated tufa that occurs at and below 1180 m in the low-elevation tufa mounds and at 1205 m in the Winnemucca Lake subbasin.

1. Introduction

1.1. Previous work

Previous studies of the Lahontan lake-level record primarily utililized the ^{14}C ages and elevations of samples of dense tufa coatings located far from suspected sites of ground-water discharge (Benson, 1993 and references therein). This procedure was implemented to avoid samples that had incorporated radioactively "dead" carbon or secondary "modern" carbon. The first form of contamination occurs when old ground water mixes with modern lake water to form a calcium carbonate precipitate; the second form of contamination occurs when modern carbon is added to a porous carbonate by a dissolution–reprecipitation process. The choice of only dense carbonates had one major shortcoming: i.e., dense tufa coatings are not distributed over the entire elevational range previously occupied by Lake Lahontan.

The sequence of formation and elevational

0031-0182/95/$9.50 © 1995 Elsevier Science B.V. All rights reserved
SSDI 0031-0182(94)00103-0

distribution of carbonates in the Pyramid Lake subbasin were discussed in part 1 of this series (Benson, 1994). The most complete sequences of tufas are found in mound-like carbonate deposits that border the shore of Pyramid Lake. The sequence of tufa formation displayed in these mounds is (from oldest to youngest): (1) a beachrock containing carbonate-cemented volcanic cobbles, (2) broken and eroded *old* spheroids that contain thinolitic tufa and an outer rind of dense laminated tufa, (3) large cylindrical (tubular) tufas capped by (4) coatings of *old* dense tufas and (5) several generations of *old* branching tufa commonly associated with thin, platy tufas and coatings of thinolitic tufa, (6) *young* spheroids that contain poorly oriented *young* thinolitic tufa in the center and several generations of radially oriented *young* thinolitic tufas near the outer edge, (7) a transitional thinolite-to-branching tufa, (8) two or more layers of *young* branching tufa, (9) a 0.5-cm thick layer of fine-grained dolomite, (10) a 2-cm thick layer of *young* dense laminated tufa, (11) a 0.1-cm thick layer of encrusting tufa that was covered by a beach deposit and (12) a 1.0-cm thick layer of porous encrusting tufa that coated the beach deposit and the sides of tufa mounds (See figs. 29 and 35 in Benson, 1994).

The purposes of this study are: (1) to determine the time interval over which each variety of tufa was deposited, (2) to construct a more detailed lake-level record for the Pyramid Lake subbasin for the past 30,000± yr, (3) to deduce the position of the southern branch of the polar jet stream from the lake-level reconstructions, and (4) to compare Lahontan and Bonneville lake-level reconstructions.

In order to accomplish these purposes, this study incorporates 221 ^{14}C ages of carbon bearing materials from the Lahontan basin including: 115 previously unpublished ^{14}C ages (including 74 AMS ^{14}C ages) of mound and other tufa complexes from the Pyramid Lake subbasin, 4 previously unpublished AMS ^{14}C ages of roots associated with tufa mounds, 59 previously published ^{14}C ages of dense tufas from the Lahontan basin (Benson, 1993 and references therein), and 43 previously published ^{14}C ages of organic materials from the Pyramid Lake and Winnemucca Lake subbasins (Thompson et al., 1986; Benson et al., 1992).

1.2. Definitions and terms

For the purposes of this paper, *Lake Lahontan* refers to any body of water existing in the Pyramid Lake subbasin prior to 10,000 yr B.P. *Western Lahontan subbasins* include the Pyramid Lake, Winnemucca Dry Lake, Smoke Creek-Black Rock and Honey Lake subbasins (Fig. 1). A *sill* is the lowest part of a divide that separates adjoining subbasins; a sill functions as a spill point when the lake in one subbasin spills to another subbasin. Change in *effective wetness* (ΔW_{eff}) necessary to achieve or exceed a sill elevation at steady state is defined as:

$$\Delta W_{\text{eff}} \equiv A_{\text{paleo}}/A_{\text{hist}} \quad (1)$$

where A_{paleo} is the paleolake surface area and A_{hist} is the mean historical surface area (corrected for anthropogenic effects). This quantitative definition of effective wetness is equivalent to the normalization of paleo-lake surface areas introduced by Benson and Paillet (1989).

Tufa *varieties* are classified as dense laminated, thinolitic, branching, and porous encrustations. Extensive tufa accumulations are divided into the following *forms*: carbonate-cemented debris (beachrock, cemented talus and cemented terraces), girdles, mounds, reefs, sheets and pendant sheets. Photographs showing examples of tufa variety and forms can be found in Benson (1994). The first occurrence of a tufa variety is termed *old* and the second occurrence is termed *young*.

Radiocarbon ages are specified as yr B.P. (years before present) and percent modern carbon is abbreviated as *pmc*. A sample that contains *dead carbon* has a ^{14}C:C ratio less than modern; e.g., old ground water is said to contain *dead carbon*. If the ^{14}C activity of a sample is at the limit of detection, the sample is said to have an *infinite* age (with respect to the method of detection).

1.3. Methods

Sample elevations (accurate to within ±3 m) were obtained by hand leveling from known eleva-

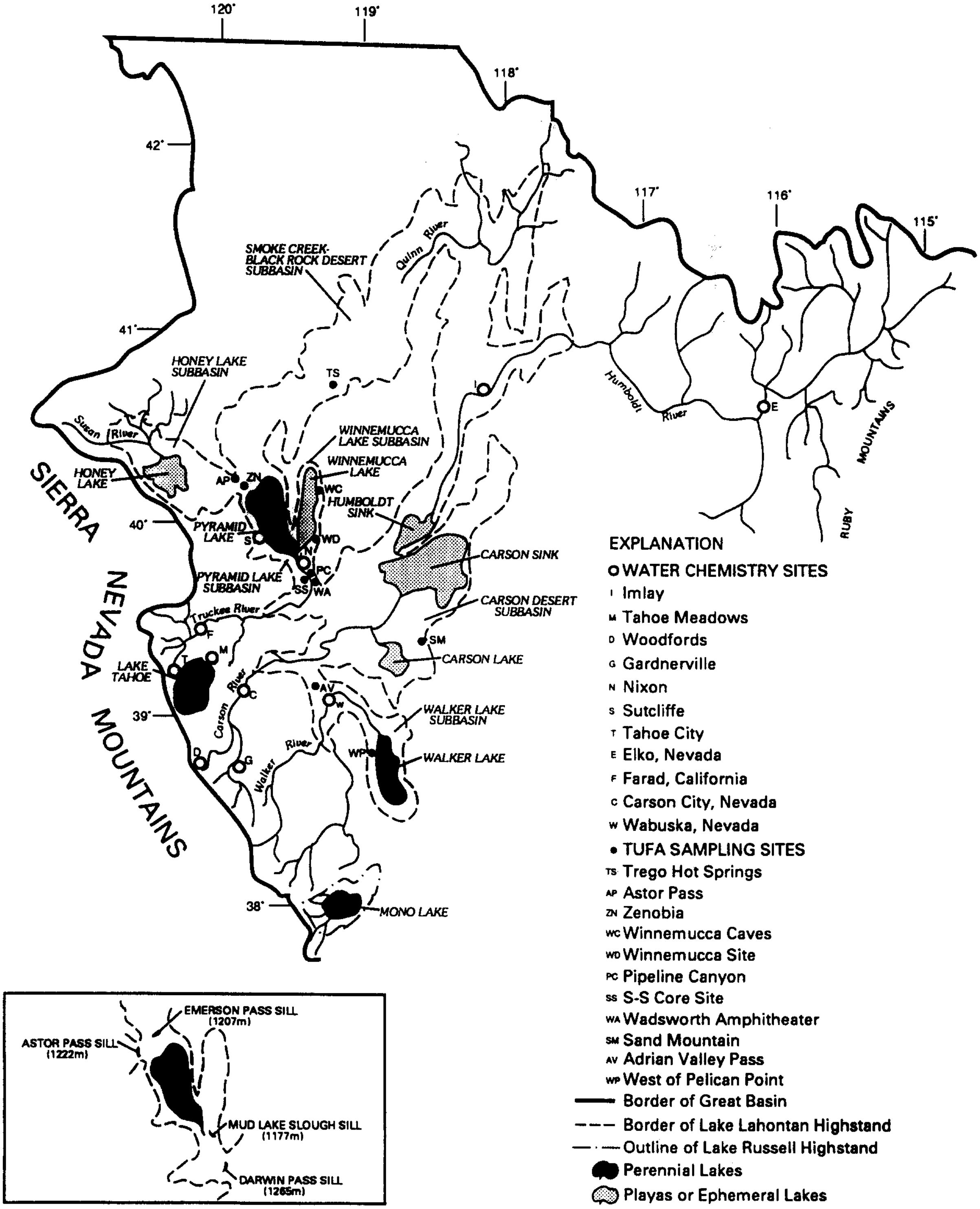

Fig. 1. Surface-water drainage for the Lahontan basin, showing location of chemistry (open circles) and tufa (filled circles) sampling sites.

tions and with the use of a digital barometer/altimeter referenced to a known elevation. Radiocarbon ages having a CAMS prefix are AMS ^{14}C dates obtained at the Center for Accelerator Mass Spectrometry at the Lawrence Livermore National Laboratory. All other previously unpublished radiocarbon ages were obtained by conventional counting techniques at the U.S. Geological Survey Radiocarbon Laboratory located in Reston Virginia. Ages of materials used to reconstruct lake levels are $\delta^{13}C$-normalized radiocarbon ages, calculated according to the guidelines given in Stuiver and Polach (1977). Tufa $\delta^{13}C$ analyses were performed at the University of Michigan and at the University of Colorado. The precision of the analyses was generally $\leqslant 0.1‰$ and is reported relative to PDB (PeeDee Belemnite). The outer surface of each tufa sample was removed in order to eliminate surficial contamination. The densest part of each tufa was selected for AMS^{14}C dating. Low-elevation (<1183 m) tufas were taken from areas that had remained covered with lake sediment until the mid 1980s and had, thereby, escaped secondary cementaion. Lao and Benson (1988) previously demonstrated that Lahontan tufa ^{14}C ages in excess of 20,000 yr should be considered unreliable. In this study, three procedures were employed to test the reliability of ^{14}C ages of the older tufas: (1) at least two dates were obtained on each tufa sample; (2) samples of the same tufa were obtained from different locations; and (3) stratigraphic consistency of ^{14}C ages was evaluated. Samples of woody material were acid and base leached to remove soluble carbonate and decomposed organic materials prior to ^{14}C age determination.

1.4. Surface-water hydrology and hypsography of the Lahontan basin

The Lahontan basin consists of seven subbasins, six of which receive discharge from perennial rivers (Fig. 1). Four of the rivers (Carson, Truckee, Walker and Humboldt Rivers) contribute ~96% of the total gaged surface inflow to the basin (Table 1). Mean-annual discharges of rivers emanating from the Sierra Nevada (Carson, Susan, Truckee, and Walker Rivers) are well correlated, but discharge of the Humboldt and Quinn Rivers is poorly correlated with Sierran discharge (Benson and Paillet, 1989). Diversion of some of these rivers may have played a role in regulating lake levels in Lahontan subbasins in the past; e.g., King (1978) and Davis (1978, 1982) described geomorphic evidence for late Quaternary diversion of the Walker and Humboldt Rivers.

Table 1
Streamflow statistics for rivers that discharge to the Lahontan basin. Data taken from Benson and Paillet (1989)

River	Mean discharge ($km^3\ yr^{-1}$)
Carson	0.454
Humboldt	1.009
Quinn	0.036
Susan	0.085
Truckee	0.725
Walker	0.379

There are seven sills within the Lahontan basin, including four sills that border the Pyramid Lake subbasin (Fig. 1). In the past, the level of Pyramid Lake was often regulated by spill to an adjacent subbasin. In addition the amount and direction of spill (out of or into the Pyramid Lake subbasin) was dependent on sill elevation, subbasin geometry and the amount of water discharged to each of the subbasins (Benson and Paillet, 1989). Therefore, it is not always possible to associate a unique value of ΔW_{eff} for a given lake elevation (surface area).

2. Radiocarbon ages of surficial carbon-bearing materials from western Lahontan subbasins

2.1. Reliability of radiocarbon ages

As discussed in previous papers (e.g., Benson, 1993), there are two principal sources of error in ^{14}C ages of Lahontan carbonates (Table 2): low initial $^{14}C/C$ ratios in lake water (reservoir effect), and addition of modern carbon after precipitation of a carbonate (open system effect). In terms of the reservoir effect, Broecker and Walton (1959) found that modern (1957) materials in Pyramid

Table 2

Elevations, radiocarbon ages, $\delta^{13}C$, and $\delta^{18}O$ values of carbonate deposits (tufas) from the Lake Lahontan basin [MB= Marble Bluff, DH= Doghead Rock, NR= Needles Rocks, PP= Pelican Point, PR= Popcorn Rocks, ZN= Zenobia, BT= Blanc Tetons, AP= Astor Pass, WC= Winnemucca Caves, SM= Sand Mountain, PC= Pipeline Canyon, TS= Trego Hot Springs–Black Rock Desert, TH= Terraced Hills, AV= Adrian Valley Pass, WP= mountain west of Pelican Point in the Walker Lake subbasin, SS= Truckee River Canyon N of S-S Ranch, WA= Wadsworth Amphitheater on east side of Truckee River Canyon N of town of Wadsworth, Nevada, WD= outcrop in southeast corner of Winnemucca Dry Lake subbasin, PI= shore due E of Pyramid Island, IR= Indian Head Rock, –= no data; if no $\delta^{13}C$ analyses were available, the $\delta^{13}C$ value of tufa was set to 3.20‰ and the $\delta^{13}C$ value of organic material was set to –25‰

Sample number	Laboratory number	Locality	Elevation (m)	^{14}C age (yr B.P.)	±	$\delta^{13}C$ (‰)
Tufa cementing talus						
PL88-1	LDGO-1723B	MB	1212	33,200	1660	(3.20)
PL88-2	LDGO-1723C	MB	1212	50,390		(3.20)
Tufa lining cave						
PL89-20b1	CAMS-5766	MB	1204	40,960	2270	3.05
Tubular tufa						
PL90-103	W-6321	DH	1218.2	18,060	180	2.49
PL91-502	W-6390	DH	1217.5	20,680	220	3.03
PL91-501	W-6389	DH	1216.4	21,190	320	2.63
PL90-102	W-6325	DH	1216.9	21,910	290	2.99
PL90-114	CAMS-5723	NR	1183	29,720	590	3.54
PL90-114	CAMS-6230	NR	1183	30,880	470	3.54
PL90-116	CAMS-5724	NR	1190	31,640	640	3.43
PL90-116	CAMS-6231	NR	1190	32,410	560	3.43
PLPP92-9	CAMS-6239	PP	1162	31,580	530	3.42
PLPP92-9	CAMS-5925	PP	1162	34,340	1260	3.42
PLPR92-2l	CAMS-3868	PR	1162	37,220	860	3.20
PLPR92-2i	CAMS-3865	PR	1162	39,060	1130	3.76
PLPR92-2k	CAMS-3867	PR	1162	40,190	1240	3.75
PLPR92-2j	CAMS-3866	PR	1162	41,380	1500	3.52
Old branching tufa						
PLPR92-1	CAMS-6241	PR	1161	17,290	140	3.04
PLPR92-1	CAMS-5927	PR	1161	19,630	140	3.04
PLPP92-7	CAMS-6234	PP	1162	19,150	120	3.34
PLPP92-7	CAMS-5924	PP	1162	20,360	130	3.34
PLPP92-1	CAMS-6233	PP	1162	20,200	140	3.31
PLPP92-1	CAMS-5923	PP	1162	20,770	130	3.31
PLPP92-6t	W-6445	PP	1162	26,020	400	3.60
PLPP92-6t	CAMS-5914	PP	1162	26,250	630	3.60
PLPPB92-1	CAMS-5926	PP	1162	27,380	270	4.21
PLPPB92-1	CAMS-6240	PP	1162	27,840	320	4.21
PLPP92-5t	CAMS-5731	PP	1162	34,130	890	2.99
PLPP92-5t	CAMS-6237	PP	1162	35,170	850	2.99
Wood coated by *old* branching tufa						
PLPP92-6W	CAMS-5683	PP	1162	29,820	520	(–25)
PLPP92-6W	CAMS-6557	PP	1162	31,410	620	(–25)
PLPP92-5W	CAMS-5682	PP	1162	37,730	1350	(–25)
PLPP92-5W	CAMS-6558	PP	1162	45,430		(–25)

Table 2 (*continued*)

Sample number	Laboratory number	Locality	Elevation (m)	^{14}C age (yr B.P.)	± (yr B.P.)	δ^{13}C (‰)
Young thinolite tufa						
PL90-109a	CAMS-5719	BT	1160	20,150	160	2.73
PLPP92-2	CAMS-6017	PP	1162	20,770	170	2.93
Young thinolite–*young* branching tufa transition						
PL90-109d	CAMS-5720	BT	1160	17,580	170	2.61
Young branching tufa (includes stony, nodular, mammillary and conal tufas found in pillow- and reef-form tufa)						
PL91-601b	CAMS-5771	MB	1251	12,110	70	4.00
PL91-601b	W-6429	MB	1251	12,560	130	4.00
PLBT92-b1a	CAMS-4425	BT	1160	12,520	90	3.15
PLBT92-b1b	CAMS-4426	BT	1160	12,730	90	3.15
PL91-503w	CAMS-5768	DH	1217.4	12,590	90	3.35
PL91-503g	CAMS-5769	DH	1217.4	13,020	90	3.35
PL91-503	W-6391	DH	1217.4	13,240	220	3.63
PLBT93-1e1	CAMS-5774	BT	1159	12,770	90	3.50
PL90-111	CAMS-5722	BT	1160	12,810	80	3.72
PL91-504	CAMS-5770	DH	1216.8	12,910	80	3.62
PL91-504	W-6393	DH	1216.8	12,980	150	3.62
PLBT92-b2b	CAMS-4428	BT	1160	12,930	90	3.10
PLBT92-b2a	CAMS-4427	BT	1160	12,940	90	3.50
PL91-602	W-6430	MB	1251	13,000	150	3.59
PL89-8	LDGO-1743p	MB	1251	13,240	80	3.54
PL89-7	LDGO-1743o	MB	1251	13,390	80	3.37
PL90-108	CAMS-6236	MB	1251	13,440	90	3.34
PL90-108	CAMS-6235	MB	1251	13,460	100	3.34
PLBT93-1e2	CAMS-5775	BT	1159	13,460	90	3.52
PL91-601a	W-6428	MB	1251	13,810	140	3.79
PL91-603	W-6431	MB	1251	14,180	150	3.72
PL90-110	CAMS-5721	BT	1160	15,730	140	2.44
PL91-604w	CAMS-5918	MB	1251	15,760	110	3.37
PL91-604g	CAMS-5917	MB	1251	17,510	150	3.37
PL91-604	W-6432	MB	1251	17,950	250	3.37
PL90-107	W-6330	DH	1220.7	15,770	190	3.01
PL90-106	W-6323	DH	1217.5	16,140	100	3.52
PL91-605	W-6433	MB	1251	16,600	220	3.52
PL91-505	W-6394	DH	1218.7	16,700	210	3.14
PL91-606	W-6434	MB	1251	16,710	220	3.45
PL91-506	W-6395	DH	1216.9	17,060	200	3.32
PL88-4	LDGO-1723e	MB	1234	17,110	190	(3.20)
PL90-101	W-6324	DH	1216.3	17,850	130	3.10
PL90-105	W-6322	DH	1218.5	18,130	150	2.85
PL89-5	LDGO-1743n	MB	1251	18,150	140	3.08
PL90-104	W-6328	DH	1217.1	18,840	220	2.96
PL88-3	LDGO-1723d	MB	1234	18,880	240	(3.20)
Chara deposits						
PL85-2c	USGS-2171	AP	1257	14,640	160	(3.20)
PL4c	I-9479	AP	1256	17,680	270	(3.20)
WDL84-3c	CL-4254140	WC	1230	18,250	220	(3.20)
PL5c	I-9480	AP	1257	18,250	290	(3.20)

Table 2 (*continued*)

Sample number	Laboratory number	Locality	Elevation (m)	^{14}C age (yr B.P.)	± (yr B.P.)	$\delta^{13}C$ (‰)
PL85-4c	USGS-2173	AP	1255	18,680	90	(3.20)
PL3c	I-9470	AP	1254	19,350	330	(3.20)
PL85-5c	USGS-2174	AP	1254	19,520	90	(3.20)
Gastropods in *Chara* deposits						
WDL84-2g	CL-4254142	WC	1230	17,540	270	−2.00
WDL84-3g	CL-4254144	WC	1230	18,180	640	−1.90
WDL84-4g	CL-4254143	WC	1230	18,410	300	−1.80
Miscellaneous dense tufa coatings from between 1207 and 1308 m						
BR84-9	CL-4240158	TS	1295	13,010	230	3.67
CD84-7	CL-4240179	SM	1303	13,130	150	3.66
PL112	I-10026	PC	1303	13,360	200	3.70
PL111	I-10025	MB	1277	13,570	200	3.71
BR84-8	CL-4240157	TS	1270	14,560	180	3.50
BR84-5	CL-4240154	TS	1238	15,970	160	2.96
PL18	I-9328	TH	1267	16,980	250	3.30
BR84-7	CL-4240156	TS	1254	17,360	260	2.67
PL89-23	W-6333	TH	1255	17,650	150	2.30
PL110	I-10019	MB	1256	17,770	270	3.12
PL15	I-9331	TH	1231	17,780	270	3.51
PL89-22	W-6332	TH	1263	18,090	180	2.12
BR84-6	CL-4240155	TS	1245	18,490	440	2.96
PL17	I-9329	TH	1260	19,040	320	2.89
PL109	I-9991	MB	1242	19,550	340	3.33
PL23	I-9342	TH	1258	19,980	360	3.57
PL44d	I-9549	TH	1258	19,980	360	2.86
BR84-4	CL-4240153	TS	1231	19,990	360	3.41
PL108	I-10018	MB	1235	20,460	380	3.17
PL44b	I-9546	TH	1258	20,650	390	3.08
PL16	I-9330	TH	1238	21,830	450	3.39
BR84-2	CL-4240151	TS	1219	23,200	400	3.15
Dense tufa coatings from above 1308 m						
PLPC92-1	CAMS-5930	PC	1325	12,490	80	3.46
PLPC92-3o	CAMS-5931	PC	1329	12,550	80	3.46
PLPC92-3i	CAMS-5932	PC	1329	12,840	70	3.39
PL103	I-10002	PC	1321	13,010	190	3.45
PL102	I-10001	PC	1312	13,040	190	3.38
PL21	I-9326	TH	1325	13,090	190	3.69
PL113	I-10028	PC	1326	13,090	190	3.52
AV84-2	CL-4240160	AV	1324	13,160	150	3.51
PL104	I-10003	PC	1321	13,320	200	3.50
BR85-2	USGS-2168	TS	1332	13,350	60	2.71
PL105	I-10004	PC	1324	13,520	200	3.40
PL101	I-10000	PC	1312	13,600	200	3.60
WL101	I-9988	WP	1330	13,810	210	(3.20)
PL41	I-9344	PC	1311	13,890	210	3.00
PL20	I-9325	TH	1311	14,030	210	3.80
PL100	I-9992	PC	1312	14,290	220	3.60
BR85-1	USGS-2169	TS	1308	14,330	60	3.72

Table 2 (*continued*)

Sample number	Laboratory number	Locality	Elevation (m)	^{14}C age (yr B.P.)	± (yr B.P.)	$\delta^{13}C$ (‰)
Tufas embedded in lake sediment						
PLLB91-2	W-6336	SS	1262	12,800	140	3.67
PLLB91-3	CAMS-5915	SS	1262	12,900	80	3.51
PLLB91-3	W-6335	SS	1262	12,960	150	3.51
PL87-2b	LDGO-1705b	WA	1230	13,330	160	3.89
PL87-2a	LDGO-1705a	WA	1230	13,380	150	2.59
PL87-2a	CAMS-5764	WA	1230	13,870	90	2.59
PL45	I-9534	WA	1262	14,250	220	3.72
Sucrosic tufa (dolomite)						
PLBT93-1d	CAMS-5773	BT	1159	11,580	80	3.51
PLBT92-d1b	CAMS-4424	BT	1160	12,030	110	3.19
PLBT92-d2a	CAMS-6242	BT	1160	12,040	80	3.19
PLBT92-d2b	CAMS-4422	BT	1160	12,260	90	3.19
PLBT92-d1a	CAMS-4423	BT	1160	12,270	120	3.19
PLBT92-d2a	CAMS-4421	BT	1160	12,370	110	3.19
Young dense laminated tufa						
PL90-1a	LDGO-1748a	BT	1163	9020	70	0.84
PLBT93-1a	CAMS-5905	BT	1159	9660	70	0.49
PLBT93-1f1	CAMS-5907	BT	1159	9770	80	0.86
WDL89-5a	CAMS-4430	WD	1205	9860	80	1.65
PL90-1b	LDGO-1748b	BT	1163	9930	80	0.84
PL90-2a	LDGO-1748c	BT	1161	9960	80	0.81
PLBT93-1f2	CAMS-5908	BT	1159	9970	70	0.56
WDL89-5b	CAMS-4431	WD	1205	9990	80	0.44
PLBT93-1b	CAMS-5906	BT	1159	10,170	70	0.64
PL90-2b	LDGO-1748d	BT	1161	10,180	80	0.81
PL87-1	LDGO-1705a	PI	1164	10,300	120	(3.20)
PLBT92-s1a	CAMS-4419	BT	1160	10,450	70	0.48
WDL89-5c	CAMS-4432	WD	1205	10,540	80	1.26
PLPI93-5a	CAMS-5909	PI	1162	10,560	70	1.10
PLBT93-1c	CAMS-5772	BT	1159	10,610	70	1.39
PLBT92-s1b	CAMS-4420	BT	1160	10,620	80	2.61
PLPI93-5b	CAMS-5910	PI	1162	10,670	70	1.92
PLPI93-5d	CAMS-5912	PI	1162	10,920	100	0.63
PLPI93-5c	CAMS-5911	PI	1162	10,960	80	2.03
Encrusting tufa						
PLBT91-9	CAMS-5725	BT	1175	2100	60	5.11
PLBT91-7	CAMS-5727	BT	1168.1	2620	60	5.16
PLBT91-8	CAMS-5726	BT	1171.2	2830	60	5.32
PLBT91-6	CAMS-5728	BT	1167.9	3450	60	5.68
PLBT91-4	CAMS-5729	BT	1166	5080	60	4.85
Beachrock						
PL40	I-9347	PR	1170	1350	70	3.98
PLND92-1	CAMS-6014	NR	1177	1890	60	2.76
PL107	I-10016	IR	1182	2110	100	4.36
PL89-2	LDGO-1743b	IR	1179	2500	30	3.48
PL89-1	LDGO-1743a	IR	1177	2510	30	4.12

Table 2 (*continued*)

Sample number	Laboratory number	Locality	Elevation (m)	^{14}C age (yr B.P.)	± (yr B.P.)	$\delta^{13}C$ (‰)
PL89-3	LDGO-1743c	IR	1182	2640	30	3.37
PL106	I-10016	IR	1179	3590	90	4.22
Tufas associated with existing springs						
PLND92-3	CAMS-5929	NR	1171	820	80	4.76
PLPYR92-1	CAMS-5928	PI	1160	1950	90	−0.19

and Walker Lakes had ^{14}C ages of ~600 and ~150 yr. Calculations performed by Benson (1993) indicated that the reservoir effect should range from ~100 to ~400 yr for large lakes in the Lahontan basin, having concentrations of inorganic carbon ranging from 25 to 33 M m^{-3} (moles per cubic meter) and CO_2 exchange rates of 6–17 M m^{-2} yr^{-1} (Peng and Broecker 1980). In general, we expect that winds over Lahontan lakes were stronger and more persistent during glacial-age climates that existed prior to 12,000 yr B.P. (see e.g. fig. 2 in Hostetler and Benson, 1990). Windier conditions would have increased CO_2 exchange rates (Erickson, 1993), thereby decreasing the magnitude of the reservoir effect. However, because there are no data on the amount of carbon dissolved in paleo-lake water, the magnitude of the paleo-reservoir effect remains conjectural.

Ground-water discharge can contribute to the magnitude of the reservoir effect. Springs occur near most tufa mounds that border Pyramid Lake (Fig. 2). Cold-water springs, especially the Popcorn Rocks and Pelican Point springs, contain relatively large concentrations of inorganic carbon (Table 3). Measurement of the ^{14}C activities of the cold and hot springs have not been made, but the ^{14}C age (1950±90 yr B.P.) of tufa recently precipitated from Pyramid Island spring (PLPYR92-1, Table 2) indicates that some tufas found at mound sites (especially the tubular tufas that seem to have been associated with ground-water discharge) probably yield ^{14}C ages that exceed the actual time of deposition.

Early petrographic studies (Benson, 1978) documented that many Lahontan tufas functioned as open systems with respect to the addition of secondary carbon. Porous tufas were found to contain visible secondary material that had been acquired in either the subaquatic or the subaerial environment. Beachrock and encrusting tufa samples included in this study usually contain multiple generations of carbonate cement; therefore, the ^{14}C ages of these samples represent an integral of more than one episode of carbonate deposition. Porous tufas from the Dog Head Rock and Marble Bluff sites (Figs. 2–4) contain areas of white secondary infill. These infillings (PL91-503w and PL91-604w) have ^{14}C ages ~400 and ~1800 yr younger than the ^{14}C ages of tufas (PL91-503g and PL91-604g) that enclose them (Table 2).

Benson and Thompson (1987), in a comparison of the ^{14}C ages of organic and inorganic carbon-bearing materials, demonstrated that tufas could acquire secondary carbon in the subaerial environment. This study determined that addition of secondary carbon, via a dissolution–reprecipitation process, occurred in some relatively dense tufas after they were subaerially exposed. Therefore, the ^{14}C ages of many tufas that have been exposed to the subaerial environment are minimum limiting estimates of their time of formation.

Some evidence, however, indicates that some tufas have remained closed systems with respect to carbon transfer. Factors that seem to support the maintenance of a closed system, are sample thickness and burial of the sample under a thick layer of impermeable sediment. The thicker the sample, the more difficult it is for secondary material to reach the sample interior. For example, samples of very old (uranium-series ages of 270,000, 185,000 and 62,000 yr B.P., Table 4) thick, dense tufas that cement talus and coat the

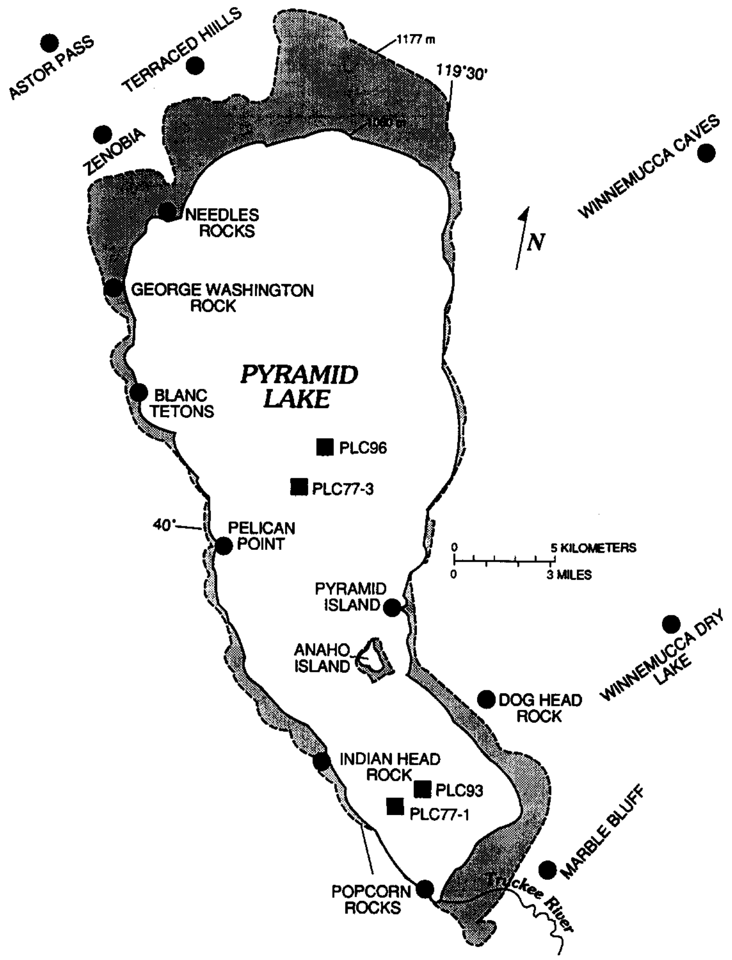

Fig. 2. Locations of tufa sampling sites (filled circles) and sediment-core sites (filled squares) in the Pyramid Lake and Winnemucca Lake subbasins.

surface of a small cave at the Marble Bluff site (see fig. 18 in Benson, 1994) have infinite radiocarbon ages (>33,000, >41,000 and >50,000 yr B.P., Table 4).

Consistency of tufa ages also indicates the maintenance of a closed system. Three highstand (1330 m) samples (WL101, 102 and 103) from the Walker Lake subbasin have identical ^{14}C ages (13,810±210, 13,760±210 and 13,760±210 yr B.P., Benson, 1993). Co-deposited samples of different mineralogy that yield the same age also indicate maintenance of a closed system. For example, dense calcite tufas and aragonite gastropods from two locations in the Pyramid Lake subbasin were shown to yield nearly identical ^{14}C ages (Benson, 1978).

Burial of tufa beneath a thick layer of sediment tends to protect the sample from contamination. The bases of many of tufa mounds (below an elevation of 1164 m) at the Blanc Teton and Pelican Point sites were covered with sediment until ~1986 and remained uncemented; e.g., the thinolite variety of tufa still consists of long porous crystals (see fig. 5 in Benson, 1994). Tufa mounds such as those at Needles Rocks (Fig. 2), however, have been exposed to lake water for several thousand years. The bases of these mounds (below an elevation of 1182 m) are densely cemented with

Table 3
Inorganic and isotopic chemistry of ground water in the Pyramid Lake system. Inorganic constituents reported in millimoles per liter; alkalinity reported as bicarbonate in millequivalents per liter; conductivity reported in millisiemens per centimeter; – = absence of data; $\delta^{13}C$ reported in parts per thousand (‰) relative to PDB; $\delta^{18}O$ and $\delta^{2}H$ reported in ‰ relative to SMOW. Samples for isotopic analysis were taken in 1992 and 1993

Site	Needles Well	Needles spring	Popcorn Rocks spring	Blanc Tetons spring	Pelican Point spring	Pyramid Island spring
Date	8/20/92	8/20/92	8/20/92	8/7/93	1977	10/7/91
pH	8.3	7.5	8.5	8.3	9.3	–
Cond.	4.47	5.51	7.60	0.62	5.45	–
T(°C)	85.3	57.8	13.0	17.0	15.5	89.0
Ca	5.7	4.3	0.21	0.043	0.081	–
Mg	0.002	1.4	2.22	0.036	1.48	–
Sr	0.057	0.046	0.0095	0.00025	–	–
Ba	0.00080	0.00073	0.00080	0.00013	–	–
Na	35.2	47.4	83.1	4.59	44.5	–
K	0.62	1.19	1.11	0.029	1.5	–
Li	0.085	0.11	0.012	0.0025	–	–
Alk.	0.24	2.04	24.7	4.68	14.0	–
Cl	52.4	62.7	73.6	1.09	32.4	–
SO_4	3.49	3.84	5.48	0.268	1.82	–
SiO_2	1.56	1.41	0.37	0.49	0.065	–
B	0.42	0.52	0.62	0.035	–	–
$\delta^{13}C$	–	−3.2	−8.2	−9.9	–	–
$\delta^{18}O$	−11.6	−12.2	−9.0	−14.6	–	−9.60
		−12.3	−9.4	−14.8		
		−12.0	−10.8			
			−9.2			
$\delta^{2}H$	−106.0	−107.5	−83.5	−113.0	–	−91.0
		−104.0	−81.0	−112.8		
		−105.5	−88.5			
			−84.5			

secondary carbonate (see figs. 9 and 13 in Benson, 1994).

Sample elevation also affects tufa preservation; i.e., the higher the elevation of a tufa sample, the less time it has spent under water. High-elevation tufas, therefore, have had less time to acquire multiple generations of carbonate cement from the subaqueous environment.

2.2. Radiocarbon ages of carbon-bearing materials from tufa mounds located near the present shore of Pyramid Lake

Tubular tufas

The insides and bases of all tufa mounds contain tubular structures. Broken tubular tufas consisting of concentric layers of dense laminated tufa[1] are exposed at the Popcorn Rocks site (Fig. 2; see fig. 15 in Benson, 1994). Radiocarbon determinations on four laminae from one of these tubes yielded ages ranging from 41,380±1500 to 37,220±860 yr B.P. (samples PLPR92-2i, j, k and l, Table 2). Ages of the three innermost samples (PLPR92-2i, j and k) are statistically identical and are ~4000 yr older than the age of the outermost layer (PLPR92-2l). All four layers are relatively porous and have ages that are essentially infinite with respect to a ^{14}C determination. It is therefore difficult, if not impossible, to assess the reliability

[1] Tubes containing branching as well as densely laminated varieties of tufa.

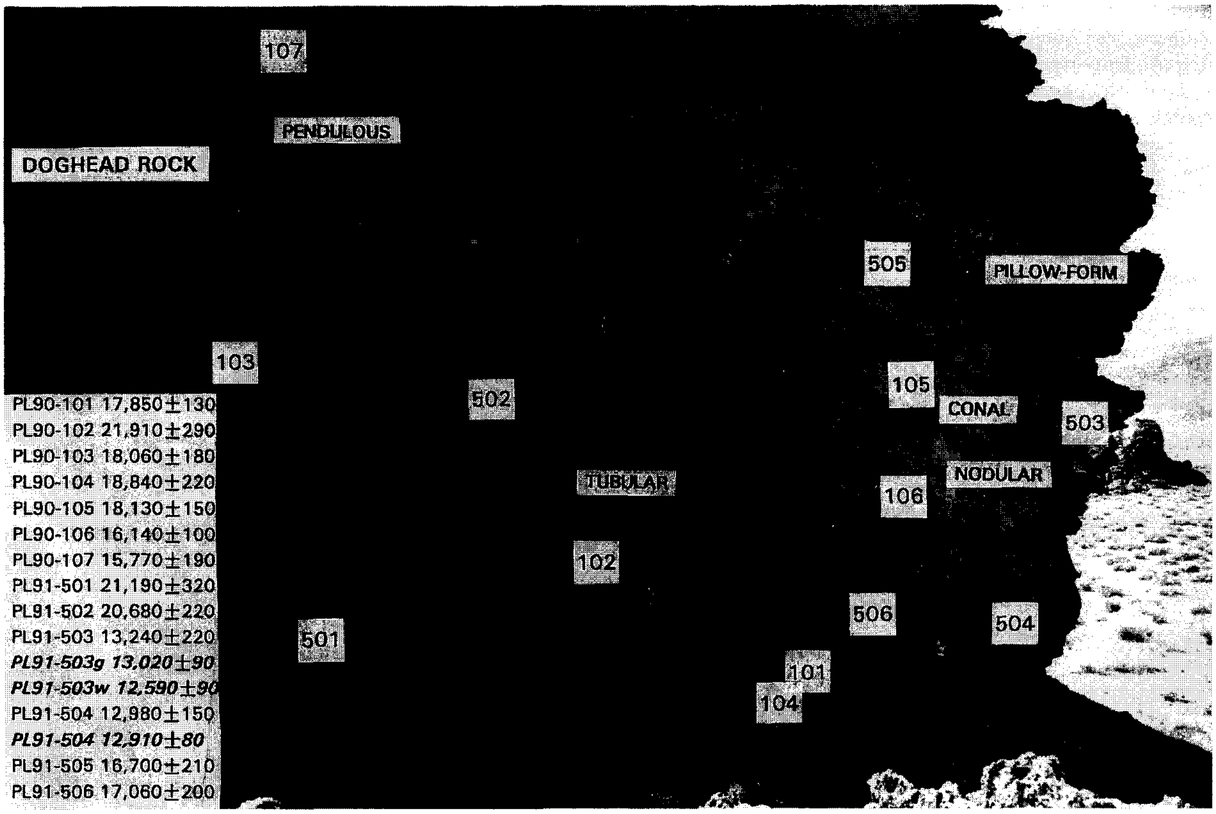

Fig. 3. Locations and radiocarbon ages of tufa samples from the Doghead Rock site. Elevation of base of outcrop is at ~1215 m. Exposed side of mound is ~5 m high. Tubular tufas are exposed in the lower center of the mound. Pillow-form, conal and nodular tufas are exposed on right side of photograph. Pendulous tufa is visible in upper left of photograph. Sample number ending in a *w* indicates white secondary carbonate cement.

of the ^{14}C ages, given the low activity of carbon remaining in the samples and the possiblity of incorporation of dead carbon during formation of the tube.

Large cylindrical tufas also are exposed at Pelican Point (Figs. 2 and 5, see fig. 26 in Benson, 1994). Two samples from the outer surface of one of the cylinders (PLPP92-9, Table 2) yielded ^{14}C ages of 34,340 ± 1260 and 31,580 ± 530 yr B.P. Two small tubular tufas from the Needles Rocks site (Fig. 2) also were dated. Samples of PL90-116[1] yielded statistically indistinguishable ^{14}C ages of 32,410 ± 560 and 31,640 ± 640 yr B.P., and samples of PL90-114 yielded similar ^{14}C ages of 30,880 ± 470 and 29,720 ± 590 yr B.P. (Table 2).

[1] Sample PL90–116 came from the base of a hive-shaped broken tufa mound that had fallen from an elevation > 1190 m.

The ^{14}C ages of low elevation (< 1207 m) tubular tufas indicate that they formed between ~35,000 and ~30,000 yr B.P. However, the shapes of the tubular tufas imply that the tubes were conduits for ground-water discharge to Pyramid Lake. Because the tubes may have formed from a mixture of lake and ground water, their ^{14}C ages should be considered maximum estimates of the time of their formation.

Old branching tufas

The Pelican Point site contains the best exposure of *old* branching tufas (Fig. 5, see figs. 12 and 26 in Benson, 1994). Radiocarbon ages of *old* branching tufa at this site ranged from 35,170 ± 850 to 19,150 ± 120 yr B.P. (Fig. 5, Table 2). The ages of carbonate casts (PLPP92-5t and PLPP92-6t)

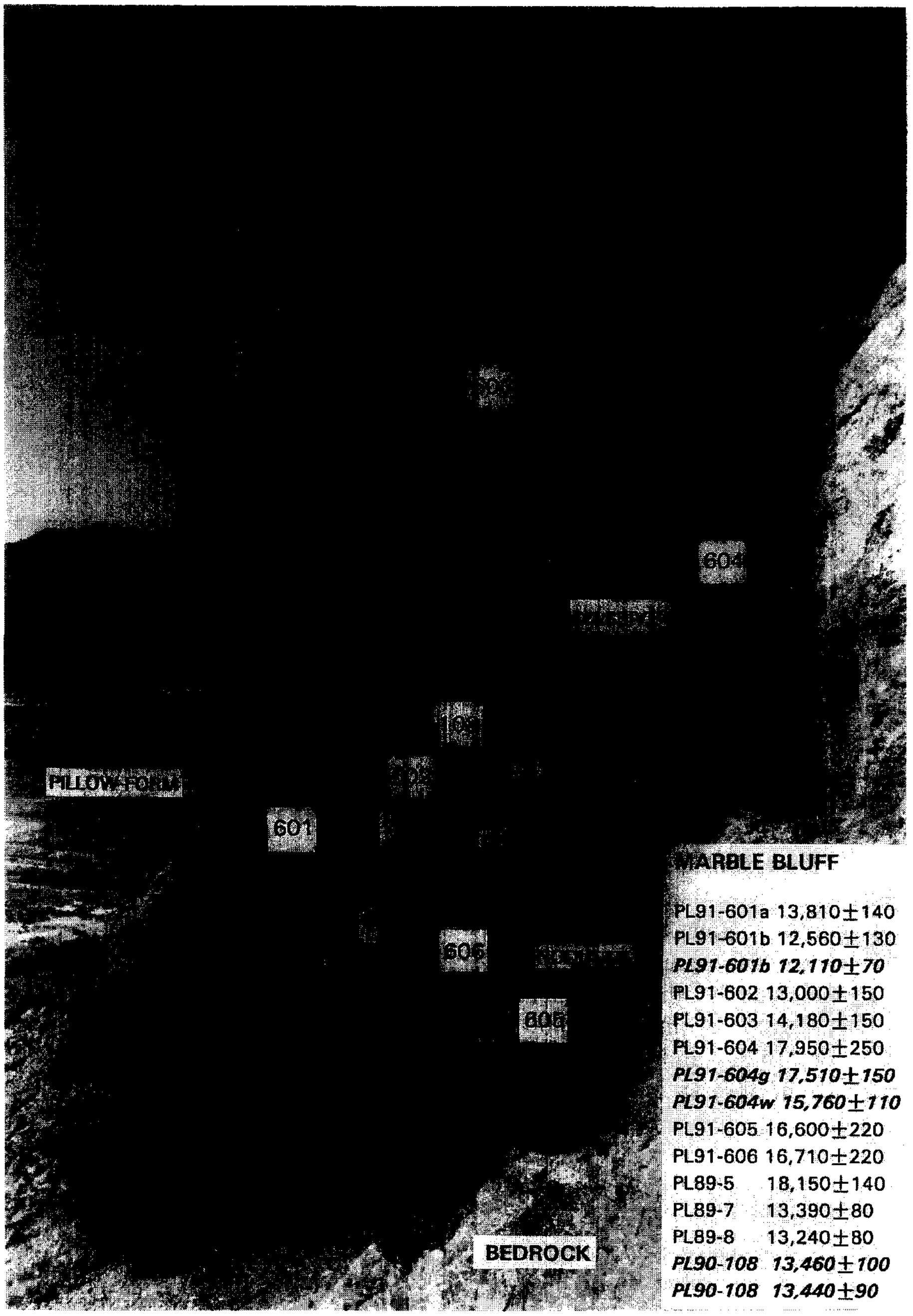

Fig. 4. Locations and radiocarbon ages of tufa samples from the Marble Bluff site. Elevation of base of outcrop is at ~1250 m. Carbonate body is 2-m wide. Inner 1 m of carbonate next to bedrock consists of massive carbonate with pockets of nodular tufa. Outer 1 m of carbonate contains overlapping pillow-form tufas that contain nodular and conal tufas. Sample numbers ending in a *w* indicate white secondary carbonate cement.

Table 4
Elevations, uranium concentrations, isotopic activity ratios and estimated uranium-series ages of dense tufa cementing talus and lining cave at Marble Bluff site in the Pyramid Lake subbasin. Letters in parentheses after sample number indicate analyst (YL = Yong Lao of Lamont-Doherty Geological Observatory and JB = James Bischoff of the U.S. Geological Survey). Slopes of $^{230}Th/^{232}Th$ versus $^{234}U/^{232}Th$ and $^{234}U/^{232}Th$ versus $^{238}U/^{232}Th$ plots of six subsamples, three each from PL88-1 and PL88-2, were used to calculate the $^{230}Th/^{234}U$ and $^{234}U/^{238}U$ ratios using the YORK-FIT program (York, 1979)

Sample number	Elevation (m)	^{238}U (ppm)	$^{234}U/^{238}U$ (Activity ratios)	$^{230}Th/^{234}U$	$^{230}Th/^{232}Th$	U-series age (10^3 yr B.P.)	^{14}C age (10^3 yr B.P.)
Tufa cementing talus							
PL88-1 (YL)	1212	1.81±0.07	1.553±0.022	0.446±0.012	–	61.8±2.3	33.2±1.7
PL88-2 (YL)		2.47±0.09					
PL89-19 (YL)	1209	5.29±0.10	1.350±0.013	0.869±0.020	19.59±0.51	187.1±11.0	>50
PL89-19 (JB)	1209	7.75±0.12	1.380±0.010	0.870±0.020	49.68±2.14	183.5±8.9	
PL89-21 (JB)	1206	2.12±0.04	1.210±0.020	0.960±0.020	36.75±2.78	269.0±29.1	
Tufa lining cave							
PL89-20a (YL)	1204	2.11±0.04	1.270±0.020	0.855±0.021	10.85±0.32	184.2±12.1	>41

found cemented to two mounds[1] are stratigraphically consistent with, but much younger than, the ages of roots (PLPP92-5w and PLPP92-6w) they enclose (Fig. 5). The gap in time between the root and cast ages (~4000–10,000 yr, Fig. 5) seems inordinately long. It is difficult to envision how dead roots could remain intact and uncoated for such long times unless they were covered and preserved by anoxic lake sediment for up to 10,000 yr. The possiblity also exists that the carbonate casts have been contaminated with secondary (modern) carbon. Given the uncertainties in the ages, we tentatively conclude that the *old* branching tufas may also have begun forming ~35,000 yr B.P. The coevality of tubular and *old* branching tufas is consistent with the observation that tubular tufas contain layers of *old* branching tufa (Benson, 1994a).

The ^{14}C ages of two samples of *old* branching tufa (PLPR92-1), deposited immediately before precipitation of the first layer of *young* thinolitic tufa at the Popcorn Rock site, differ by ~2300 yr. The oldest of the ^{14}C dates (19,630±140 yr B.P.) is similar to ^{14}C dates (20,770±170 to 19,150±120 yr B.P.) obtained on samples (PLPP92-1, PLPP92-2, and PLPP92-7) collected from the same tufa layer at Pelican Point. Because samples from Popcorn Rock are coated with white secondary carbonate, their ages represent minimum estimates of the time of final deposition of *old* branching tufa. The youngest ^{14}C age of the Pelican Point *old* branching tufas is, therefore, rejected and we conclude that *old* branching tufas continued to form until ~19,000 yr B.P.

Tufas deposited since formation of old branching tufas

Most of the tufa varieties deposited after formation of *old* branching tufa are exposed at the Blanc Tetons site (Figs. 6 and 7). The lowermost layer of *young* thinolitic tufa (PL90-109a, Table 2) at this site has a ^{14}C age of 20,150±160 yr B.P. This date is consistent with the age (20,770±170 yr B.P.) of a sample (PLPP92-2, Table 2) of the same variety of tufa taken from Pelican Point. Shearman et al. (1989) consider that ikaite, the hexahydrate of calcium carbonate, was the precursor of thinolitic tufas. The formation of ikaite indicates the presence of very cold water. In addition, high levels of dissolved orthophosphate seem necessary to prevent rapid conversion of ikaite to a more thermodynamically stable form of carbonate (Bischoff et al., 1993). Ikaite has often been found forming near the outlets of calcium-rich bicarbonate-bearing springs (Pauly, 1963; Bischoff et al., 1993) indicating that it may incorporate dead

[1] Samples PLPP92-5t and 6t came from the outer surfaces of different mounds.

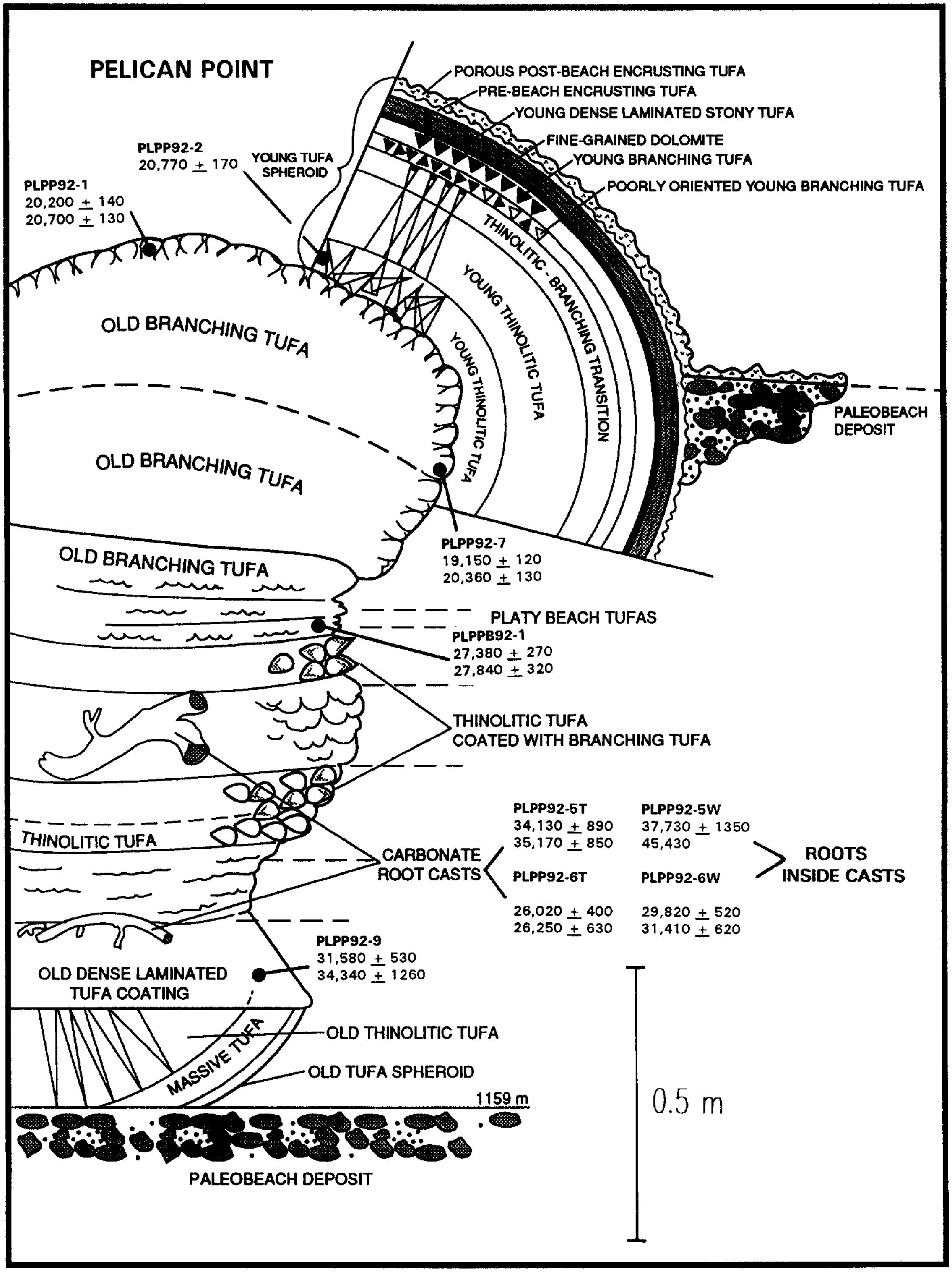

Fig. 5. Schematic sequence of tufa deposition at the Pelican Point site, showing radiocarbon ages of some tufa types. Tufa complexes at this site are typically 2–3 m in height.

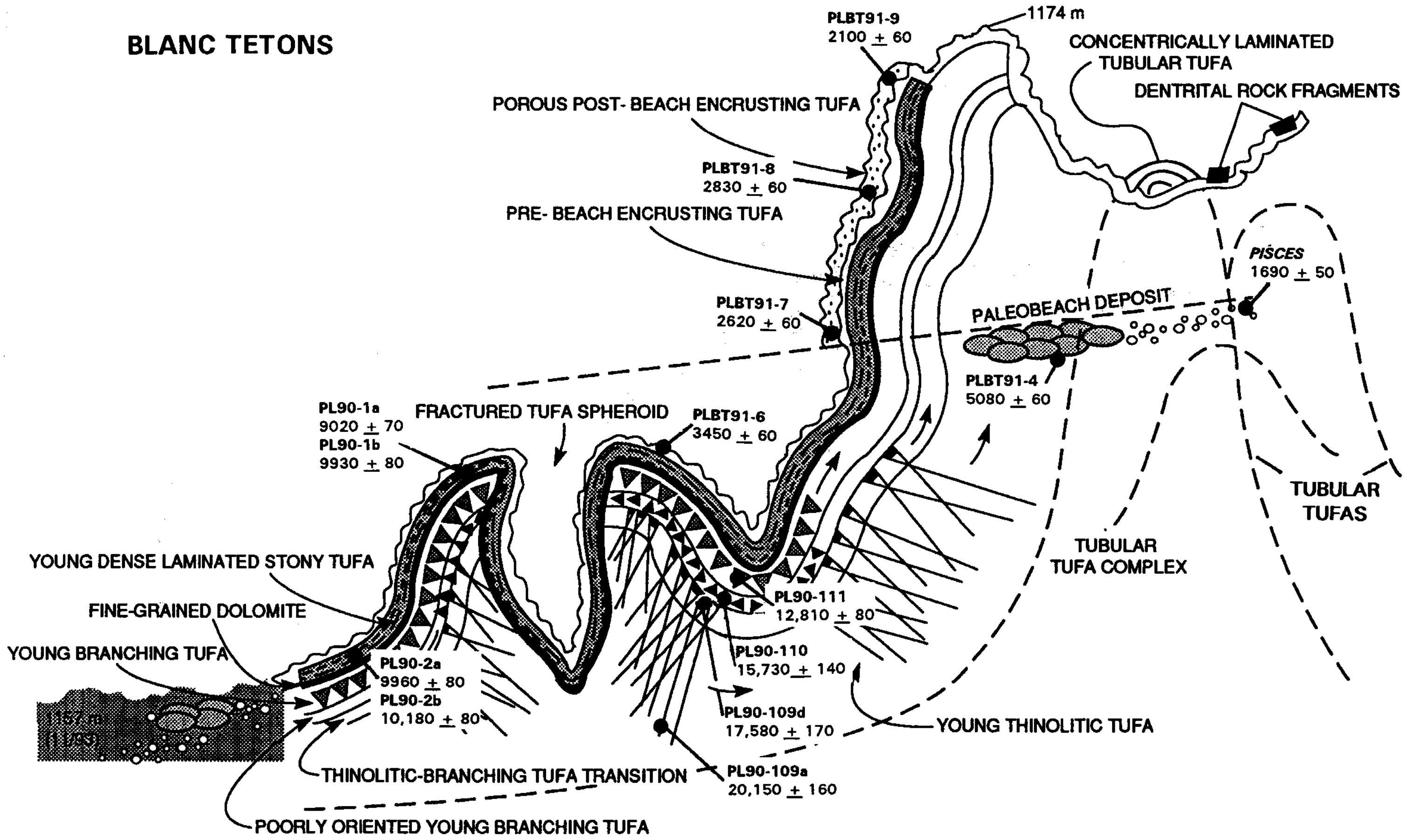

Fig. 6. Schematic sequence of tufa deposition at the Blanc Tetons site, showing radiocarbon ages of some tufa types. Mounds at this site are ~13 m high.

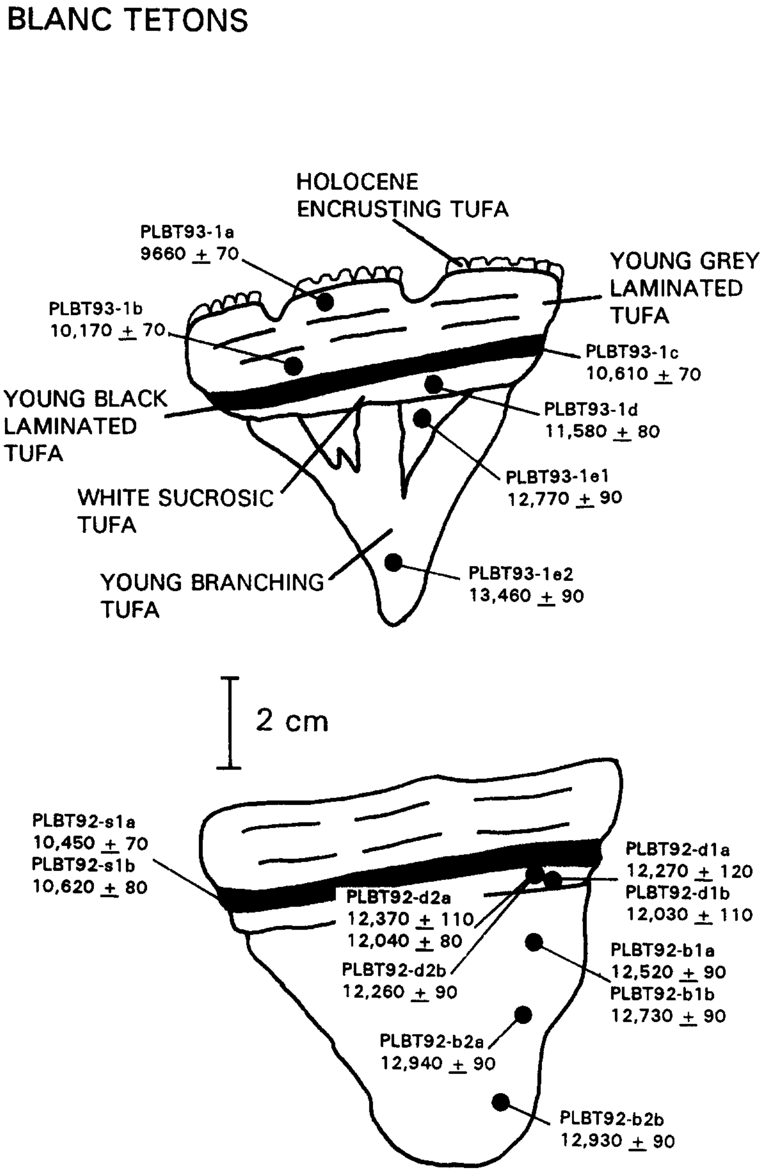

Fig. 7. Radiocarbon ages of *young* branching tufa, white sucrosic (dolomitic) tufa, and *young* laminated tufa from the Blanc Tetons site. The laminated tufa averages ~2 cm in thickness.

carbon as it forms. However, the ages of PL90-109a and PLPP92-2 are essentially the same as the ages of the last generation of *old* branching tufa coated by the thinolite. The similarity of ages is unexpected since it was thought that ikaite/thinolite would persist as the metastable hexahydrate for a lengthy period of time prior to recrystallization to a more stable carbonate. For example, Broecker and Kaufman (1965) found that thinolite contained within a tufa dome from the Needles Rocks site dated ~4000 yr younger than the branching tufa that surrounded it. It seems, however, that the thinolitic tufas at the Blanc Tetons recrystallized soon after formation. Thinolites in the bases of tufa mounds at Needles Rocks are densely cemented with secondary carbonate.

Therefore, the ^{14}C age of the Needles Rocks thinolites dated by Broecker and Kaufman (1965) probably represents the introduction of secondary carbonate cement that filled the porous thinolite framework.

The transition from *young* thinolite to *young* branching tufa (PL90-109d) at the Blanc Tetons site has a ^{14}C age of 17,580 ± 170 yr B.P. (Table 2, see fig. 31 in Benson, 1994). *Young* branching tufas at this site range in age from 15,730 ± 140 to 12,590 ± 90 yr B.P. (Table 2). Because thinolitic (ikaite) tufas are expected to have formed in very cold water, Benson (1994a) hypothesized that the *young* thinolites formed in the hypolimnetic waters of Lake Lahontan. The period of thinolite formation, therefore, indicates that Lake Lahontan was deep between ~21,000 and ~17,600 yr B.P.

After deposition of the last generation of *young* branching tufa at the Blanc Tetons site, the base of the mound was exposed by a drop in lake level accompanied by the erosion of lake sediment that previously covered the flanks of the mound. When the supporting sediment was removed, some large tufa spheroids on the flanks of the mound cracked open (see Fig. 5 in Benson, 1994a) and were subsequently coated with a 0.5-cm thick layer of sucrosic tufa (dolomite). The ^{14}C age of the dolomite ranges from 12,370 ± 110 to 11,580 ± 80 yr B.P. (Fig. 7, Table 2). The dolomite is porous, and x-ray diffraction studies of sample PLBT93-1d indicate that this sample also contains calcite. Petrographic studies indicate that the calcite was added after the dolomite formed. If we reject the age of this sample contaminated with secondary carbon, the remaining data indicate that dolomite precipitation occurred between 12,400 and 12,000 yr B.P. Because dolomite precipitation has been shown to occur in saline, alkaline lakes having a high magnesium to calcium ratio (De Deckker and Last, 1988), we infer that Lake Lahontan was at low levels (~1260 m) between 12,400 and 12,000 yr ago.

The age of a 2-cm thick *young* dense laminated tufa that overlies the dolomite at the Blanc Tetons site ranges in age from 10,960 ± 80 to 9020 ± 70 yr B.P. (Fig. 7, Table 2). Dates on this tufa at the Winnemucca Lake and Pyramid Island sites (Fig. 2, Table 2) also fall within the 11,000–9000 yr age range. The gap in tufa formation between 12,000 and 11,000 yr B.P. indicates the possibility that Lake Lahontan fell below 1259 m during this time. The *young* dense laminated tufa occurs between 1159 and 1205 m, indicating that Lake Lahontan rose after 11,000 yr B.P. reaching the spill point to the Smoke Creek-Black Rock Desert subbasin prior to 9000 yr B.P.

A thin porous tufa that encrusts carbonate cemented cobbles (see Figs. 7 and 33 in Benson, 1994) perched on the side of the Blanc Tetons mound at 1166 m (Fig. 6) has a ^{14}C age of 5080 ± 60 yr B.P. (PLBT91-4, Table 2). Thicker encrusting tufas from higher elevations (1167–1175 m) on the mound range in age from 3450 ± 60 to 2100 ± 60 yr B.P. (Fig. 6, Table 2). X-ray diffraction studies of samples of the encrusting tufa indicate that it is usually composed of aragonite and sometimes contains small amounts of dolomite, minerals that probably precipitated from relatively saline lake water. The mineralogic and elevational data indicate that Pyramid Lake was at or below the spill point to the Winnemucca Lake subbasin for most of the middle and late Holocene.

Beachrock deposits

A sandy beach deposit, containing fossil fish bones, occurs at an elevation of ~1167 m on the north side of the southern Blanc Tetons mound. The ^{14}C age of purified collagen extracted from the fish bones (CAMS-5892) is 1690 ± 50 yr B.P. Beachrock also occurs at many other sites bordering Pyramid Lake between elevations of 1170 and 1182 m (see fig. 16 in Benson, 1994). Dates on samples from these deposits range from 3590 ± 90 to 1350 ± 70 yr B.P. (Table 2). This age range is similar to ages of beach deposits and encrusting shallow-water tufas found at the Blanc Tetons site supporting our conclusion that Pyramid Lake was at or below the spill point to the Winnemucca Lake subbasin for most of the middle and lake Holocene.

2.3. Radiocarbon ages of carbon-bearing materials from tufa mounds located above 1207 m

Tufa sequences from higher elevations are generally not as complete as those from low elevations, but they do provide information on the timing and maximum vertical extent of tufa occurrence.

Dog Head Rock

The base of the eastern side of Dog Head Rock (Fig. 2) lies at an elevation of ~1215 m. At this location, the side of a hive shaped tufa mound has collapsed, exposing the central core of the mound (Fig. 3). Tubular tufas (3–5 cm in diameter) are exposed at the base of the hive shaped mound (Fig. 3, see fig. 14 in Benson, 1994). The tubes range in age from 21,910±290 to 18,060±180 yr B.P. (Table 2). Because we associate tube formation with ground-water discharge, the age of the tubes are considered maximum estimates of the times of formation. The ages of these tubes are much younger than the ages of tubes contained in mounds located along Pyramid Lake's periphery, indicating that lake level had not reached 1215 m until ~21,900 yr B.P.

Young branching tufa at Dog Head Rock includes stony, nodular, mammillary, and conal shapes that form drape and pillow structures (Benson, 1994). The ^{14}C ages of these tufas range from 18,840±220 to 12,910±80 yr B.P. (Fig. 3, Table 2) with tufa age decreasing towards the outer edge of the hive structure. The age data for tubular and *young* branching tufa imply that lake level remained above 1215 m between ~22,000 and ~12,900 yr B.P.

Marble Bluff

A reef-form tufa at 1251 m at the Marble Bluff site (Fig. 2) also contains *young* branching tufas with stony, nodular, mammillary, and conal shapes (Fig. 4). The ages of uncontaminated samples from this site range from 18,150±140 to 12,560±130 yr B.P. (Table 2). Two tufas from pillows at a lower elevation (1234 m) at Marble Bluff have ^{14}C ages of 18,880±240 and 17,110±190 yr B.P. (Table 2). The age range of these *young* branching tufas indicates that lake level remained above 1250 m between ~18,200 and ~12,600 yr B.P.

3. Sequence of formation of tufa varieties and forms

The age data presented above, together with the ages of *chara* deposits, gastropods embedded in the *chara* deposits and highstand dense coatings (Table 2), allow us to determine the sequence of formation of tufa varieties (Fig. 8). Tufa sequences have been graphed for four elevational ranges: <1182 m, 1182–1207 m, 1207–1265 m, and >1308 m. These ranges bear some relation to the hydrologic state of the the Lahontan system. When the lake surface was located below 1182 m, Pyramid Lake was hydrologically isolated from other subbasins. When the lake surface was located between 1182 and 1207 m, Pyramid and Winnemucca Lakes were joined. When the lake surface was located between 1207 and 1265 m, lakes in the Pyramid, Winnemucca and Smoke Creek-Black Rock Desert subbasins were joined. If the Humboldt River discharged to the Black Rock Desert, Carson Lake received spill from the western Lahontan lakes when they rose to 1265 m. If, however, the Humboldt River discharged to the Carson Desert subbasin, Carson Lake joined with the western Lahontan lakes when lake levels were at 1265 m. When lake surface exceeded 1308 m, lakes in all seven Lahontan subbasins coalesced (see Table 5).

The data of Fig. 8 indicate the following: (1) the lower the elevation, the greater the time over which carbonate deposition has occurred, (2) tubular tufas formed at various elevations in the Pyramid Lake subbasin, implying that the groundwater potentiometric surface was much higher in the past, (3) *old* branching tufas (and tubular tufas that contain *old* branching tufa) that formed at low elevations were succeeded by *young* thinolitic tufas, (4) *young* thinolitic tufas formed at relatively low elevations (<1220 m) at the same time that *young* branching tufa and *chara* were deposited at higher elevations, (5) dolomitic tufas precipitated from between 12,400 and 12,000 yr B.P. and aragonitic and dolomitic encrusting tufas precipitated in the latter part of the Holocene (<3450 yr B.P.), and (6) laminated fresh-water low-magnesium-calcite tufas formed between 11,000 and 9000 yr B.P.

4. The Lahontan lake-level record

A lake-level synthesis based on the data of Table 2 is shown in Fig. 9. The lake-level record prior

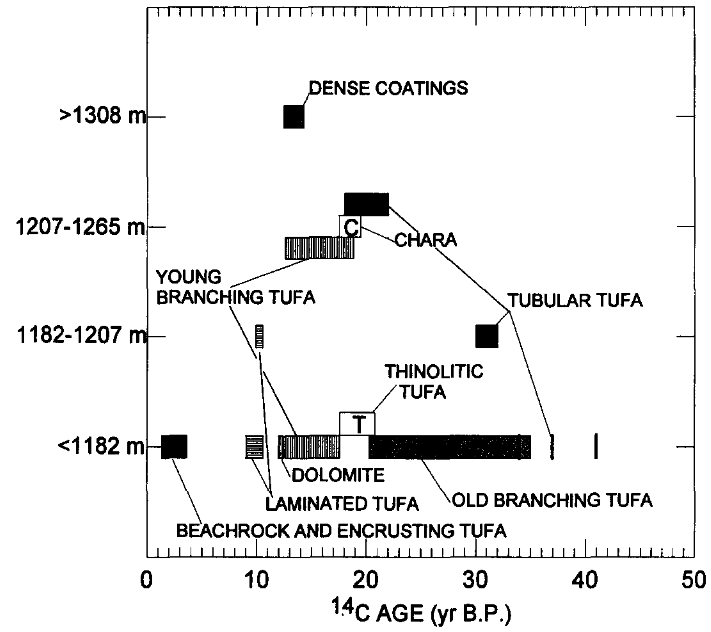

Fig. 8. Order of formation (paragenesis) of tufas in the Pyramid Lake and Winnemucca Lake subbasins shown for different elevations. Below 1182 m, Pyramid Lake is confined to the Pyramid Lake subbasin. When Pyramid Lake reaches 1183 m (Mud Lake Slough Sill), it spills to the Winnemucca Lake subbasin. Above 1207 m, the lake in the Pyramid and Winnemucca Lake subbasins spills to the Smoke Creek–Black Rock Desert subbasin across Emerson Pass Sill. When the lakes in the western Lahontan subbasins reach 1265 m, spill occurs across the Darwin Pass Sill to the Carson Desert subbasin. Above 1308 m, a single highstand lake occupies the seven Lahontan subbasins.

to 24,000 yr B.P. cannot be accurately determined from the ^{14}C ages of tubular and *old* branching tufas that formed at low elevations in association with ground-water discharge. For this reason, these tufa ages have not been included in the lake-level synthesis. The lake-level envelope between 24,000 and 1500 yr B.P. was drawn above all water-laid deposits and below all subaerial deposits. Dates on organic materials deposited between 13,000 and 9000 yr B.P. were taken from compilations in Thompson et al. (1986) and Benson et al. (1992).

4.1. 27,500–15,500 yr B.P.

The most reliable data on lake level during this period comes from ^{14}C ages of amino acids extracted from the bones of a camel skeleton (Stafford et al., 1991). Dansie et al. (1990) have presented convincing arguments supporting a shallow-water death of the camel. Stafford (pers. comm.) believes that the best estimate of the ^{14}C age of the camel is $25,870 \pm 590$ yr B.P. (AA-2663) based on the XAD-purified hydrolysate fraction extracted in weak HCL. However, the age could be as young as $23,250 \pm 360$ yr B.P. (AA-2984) based on the ^{14}C age of the hydroxyproline fraction which is endemic to bone material. The ^{14}C ages of the youngest root cast found at Pelican Point (PLPP92-6T, Fig. 5) are statistically indistinguishable from the oldest age estimate for the camel. In addition, sample PLPPB92-1 (tufa filling the eye socket of a prehistoric horse) from Pelican Point has an ^{14}C age (~27,500 yr B.P., Fig. 5) slightly older than the oldest age estimate for the camel. These data indicate that Pyramid Lake was at a low elevation (~1165 m) at least part of the time between ~27,500 and ~23,250 yr B.P. (Fig. 9). By ~21,000 yr B.P, Lake Lahontan had reached the elevation of the 1265-m sill at Darwin Pass.

The surface of Lake Lahontan seems to have remained near the elevation (1165 m) of the Darwin Pass spill point between ~20,000 and

Table 5

Change in effective wetness associated with hydrologic states experienced by the Lahontan basin in the late Quaternary. For the purposes of this table, effective wetness is defined as the ratio of streamflow discharge associated with a hydrologic state relative to mean historical streamflow discharge. Streamflow data from Table 1 together with an evaporation rate of 1.25 m yr^{-1} and surface areas listed in Table 2 were used in the calculation of effective wetness

Hydrologic state	Effective wetness
Humboldt River discharges to Carson Desert subbasin; Walker River discharges to Walker Lake subbasin	
Pyramid Lake reaches 1177 m and spills to Winnemucca Lake subbasin	0.98
Pyramid and Winnemucca Lakes coalesce at 1177 m	1.42
Lake in Pyramid and Winnemucca Lake subbasins reaches 1207 m and spills to Smoke Creek–Black Rock Desert subbasin	1.75
Walker Lake reaches 1308 m and spills to Carson Desert subbasin	2.58
Carson Lake reaches 1265 m and spills to lake in Pyramid and Winnemucca Lake subbasins; lake in Pyramid and Winnemucca Lake subbasins continues to spill to Smoke Creek–Black Rock Desert subbasin and Walker Lake continues to spill to Carson Desert subbasin	4.66
Lakes in Pyramid, Winnemucca and Smoke Creek–Black Rock Desert subbasins coalesce at 1207 m; Walker Lake continues to spill to Carson Desert subbasin and Carson Lake continues to spill to Pyramid Lake subbasin	4.99
Lake in Pyramid Lake, Winnemucca Lake and Smoke Creek–Black Rock Desert subbasins reaches 1222 m and spills to Honey Lake subbasin; Walker Lake continues to spill to Carson Desert subbasin and Carson Lake continues to spill to Pyramid Lake subbasin	5.29
Lakes in Pyramid Lake, Winnemucca Lake, Smoke Creek–Black Rock Desert and Honey Lake subbasins coalesce at 1222 m; Walker Lake continues to spill to Carson Desert subbasin and Carson Lake continues to spill to Pyramid Lake subbasin	5.37
Lake in Pyramid Lake, Winnemucca Lake, Smoke Creek–Black Rock Desert and Honey Lake subbasin reaches 1225 m; Walker Lake continues to spill to Carson Desert subbasin and Carson Lake continues to spill to Pyramid Lake subbasin	5.42
Lakes in Pyramid Lake, Winnemucca Lake, Smoke Creek–Black Rock Desert, Honey Lake, Carson Desert, and Buena Vista subbasins coalesce at 1265 m; Walker Lake continues to spill to Carson Desert subbasin	7.02
All lakes in Lahontan subbasins coalesce at 1308 m	9.24
Lake Lahontan achieves 1335-m highstand	10.59
Humboldt River discharges to Smoke Creek-Black Rock Desert subbasin; Walker River discharges to Walker Lake subbasin	
Pyramid Lake reaches 1177 m and spills to Winnemucca Lake subbasin	0.98
Pyramid and Winnemucca Lakes coalesce at 1177 m	1.42
Lake in Pyramid and Winnemucca Lake subbasins reaches 1207 m and spills to Smoke Creek–Black Rock Desert subbasin	1.75
Lakes in Pyramid, Winnemucca and Smoke Creek–Black Rock Desert subbasins coalesce at 1207 m	2.49
Walker Lake reaches 1208 m and spills to Carson Desert subbasin	2.58
Lake in Pyramid Lake, Winnemucca Lake and Smoke Creek–Black Rock Desert reaches 1222 m and spills to Honey Lake subbasin; Walker Lake continues to spill to Carson Desert subbasin	2.93
Lakes in Pyramid Lake, Winnemucca Lake, Smoke Creek–Black Rock Desert and Honey Lake subbasin coalesce at 1222 m; Walker Lake continues to spill to Carson Desert subbasin	3.16
Lake in Pyramid Lake, Winnemucca Lake, Smoke Creek–Black Rock Desert and Honey Lake subbasin reaches 1225 m; Walker Lake continues to spill to Carson Desert subbasin	3.22
Lake in Pyramid Lake, Winnemucca Lake, Smoke Creek–Black Rock Desert and Honey Lake subbasin reaches 1265 m and spills to Carson Desert subbasin; Walker Lake continues to spill to Carson Desert subbasin	5.54
Lakes in Pyramid Lake, Winnemucca Lake, Smoke Creek–Black Rock Desert, Honey Lake, Carson Desert and Buena Vista subbasins coalesce at 1265 m; Walker Lake continues to spill to Carson Desert subbasin	7.02
All lakes in Lahontan subbasins coalesce at 1308 m	9.24
Lake Lahontan achieves 1335-m highstand	10.59

Table 5

Hydrologic state	Effective wetness
Humboldt River discharges to Carson Desert subbasin; Walker River discharges to Carson Desert subbasin	
Pyramid Lake reaches 1177 m and spills to Winnemucca Lake subbasin	0.98
Pyramid and Winnemucca Lakes coalesce at 1177 m	1.42
Lake in Pyramid and Winnemucca Lake subbasins reaches 1207 m and spills to Smoke Creek–Black Rock Desert subbasin	1.75
Carson Lake reaches 1265 m and spills to lake in Pyramid and Winnemucca Lake subbasins; lake in Pyramid and Winnemucca Lake subbasins continues to spill to Smoke Creek–Black Rock Desert subbasins	4.12
Lakes in Pyramid, Winnemucca and Smoke Creek–Black Rock Desert subbasins coalesce at 1207 m; Carson Lake continues to spill to lake in Pyramid, Winnemucca, and Smoke Creek–Black Rock Desert subbasins	4.47
Lake in Pyramid Lake, Winnemucca Lake, and Smoke Creek–Black Rock Desert reaches 1222 m and spills to Honey Lake subbasin; Carson Lake continues to spill to lake in Pyramid, Winnemucca, Honey Lake and Smoke Creek–Black Rock Desert subbasins	4.76
Lake in Pyramid Lake, Winnemucca Lake, Smoke Creek–Black Rock Desert and Honey Lake subbasin coalesce at 1222 m; Carson Lake continues to spill to lake in Pyramid, Winnemucca, Honey Lake and Smoke Creek–Black Rock Desert subbasins	4.82
Lake in Pyramid, Winnemucca, Honey Lake and Smoke Creek–Black Rock Desert subbasins reach 1225 m; Carson Lake continues to spill to lake in Pyramid, Winnemucca, Honey Lake and Smoke Creek–Black Rock Desert subbasins	5.05
Lake in Pyramid Lake, Winnemucca Lake, Smoke Creek–Black Rock Desert, Honey Lake, Carson Desert and Buena Vista subbasins coalesce at 1265 m	6.65
Lake in Pyramid Lake, Winnemucca Lake, Smoke Creek–Black Rock Desert, Honey Lake, Carson Desert and Buena Vista subbasins reaches 1308 m and spills to Walker Lake subbasin	8.88
All lakes in Lahontan basin coalesce at 1308 m	9.24
Lake Lahontan achieves 1335-m highstand	10.59
Humboldt River discharges to Smoke Creek–Black Rock Desert subbasin; Walker River discharges to Carson Desert subbasin	
Pyramid Lake reaches 1177 m and spills to Winnemucca Lake subbasin	0.98
Pyramid and Winnemucca Lakes coalesce at 1177 m	1.42
Lake in Pyramid and Winnemucca Lake subbasins reaches 1207 m and spills to Smoke Creek–Black Rock Desert subbasin	1.75
Lakes in Pyramid, Winnemucca and Smoke Creek–Black Rock Desert subbasins coalesce at 1207 m	2.49
Lake in Pyramid Lake, Winnemucca Lake, and Smoke Creek–Black Rock Desert reaches 1222 m and spills to Honey Lake subbasin	2.93
Lakes in Pyramid Lake, Winnemucca Lake, Smoke Creek–Black Rock Desert and Honey Lake subbasin coalesce at 1222 m	3.16
Lake in Pyramid Lake, Winnemucca Lake, Smoke Creek–Black Rock Desert and Honey Lake subbasin reach 1225 m	3.22
Lake in Pyramid Lake, Winnemucca Lake, Smoke Creek–Black Rock Desert and Honey Lake subbasin reaches 1265 m and spills to Carson Desert subbasin	5.54
Lakes in Pyramid Lake, Winnemucca Lake, Smoke Creek–Black Rock Desert, Honey Lake, Carson Desert and Buena Vista subbasins coalesce at 1265 m	6.65
Lake in Pyramid Lake, Winnemucca Lake, Smoke Creek–Black Rock Desert, Honey Lake and Carson Desert subbasins reaches 1308 m and spills to Walker Lake subbasin	8.88
All lakes in Lahontan basin coalesce at 1308 m	9.24
Lake Lahontan achieves 1335-m highstand	10.59

~16,000 yr B.P. (Fig. 9). Inaccuracies inherent in the ^{14}C data set and our inability to determine the absolute depth of formation of most of tufas make it impossible to draw a single line that depicts actual variations in lake level during this time interval. The occurrence of a soil intercalated in

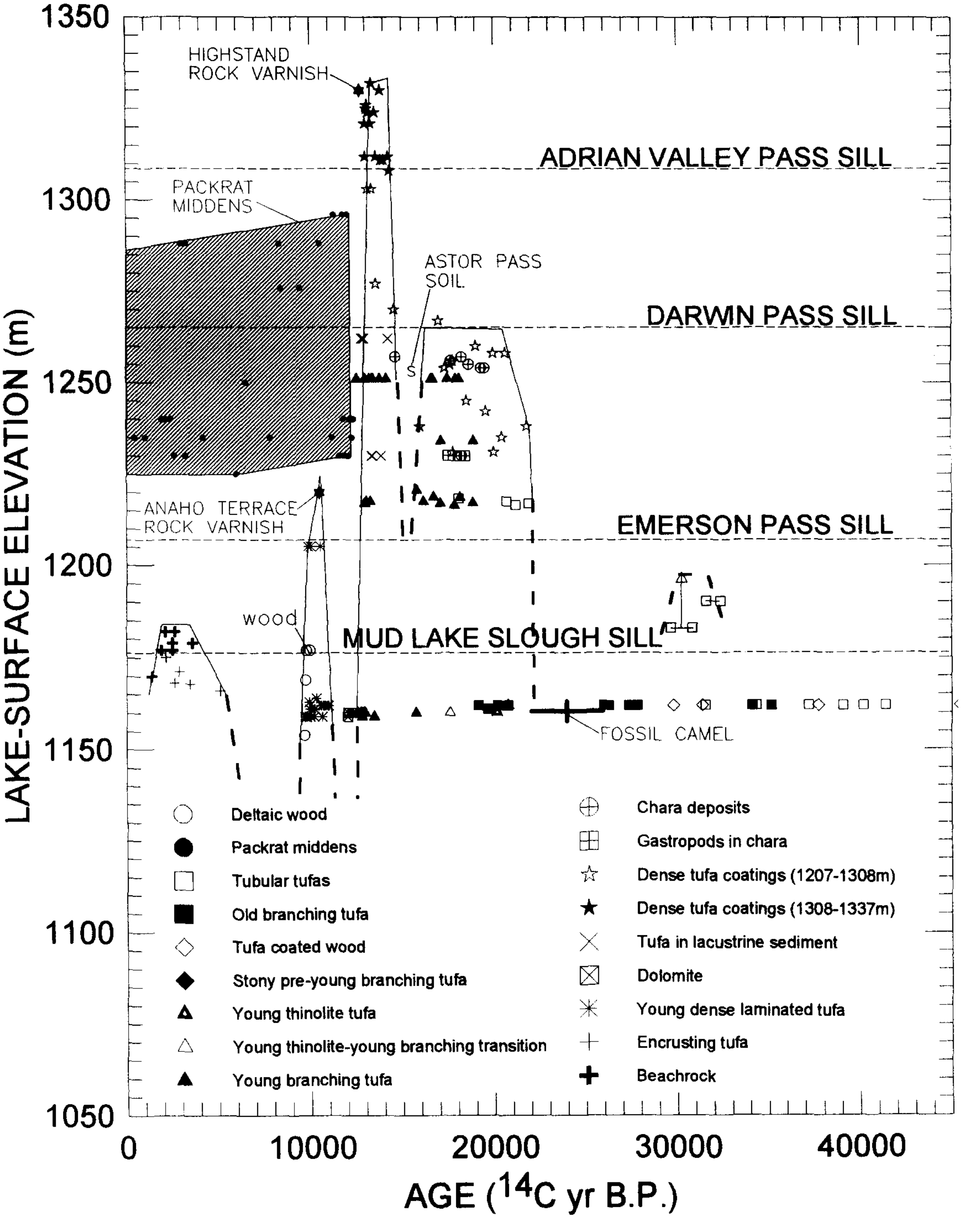

Fig. 9. Lahontan lake-level record for the past 35,000 yr. Samples from elevations < 1200 m are from tufa mounds that may have acquired radioactively dead carbon from ground water. Dashed lines indicate conjectured trajectories of lake-level rise and fall.

chara and diatom deposits in the Astor Pass area indicates a decline in lake level to <1252 m by ~15,500 yr B.P. [organic carbon from this soil (PL85-3S) has a ^{14}C age of 15,660±150 yr B.P.].

4.2. 15,500–12,400 yr B.P.

By 14,500 yr B.P., lakes in all Lahontan subbasins had reached 1308 m and coalesced; by 13,800 yr B.P., tufa was being precipitated at 1330± m. Lake Lahontan began to recede from its highstand by ~13,600 yr B.P., reaching an elevation of ~1160 m by 12,400 yr B.P. (Fig. 9).

4.3. 12,400–9000 yr B.P.

Between 12,370±310 and 12,030±110 yr B.P., dolomite precipitation occurred at low elevations (1160± m) around the Pyramid Lake subbasin. A gap in tufa deposition exists between 12,030±110 yr and 10,960±80 yr B.P. We interpret this gap as indicating that Pyramid Lake fell below 1159 m during this time interval which was coeval with the Allerod Interstade (Wright, 1989).

Between 10,960±80 and 9020±70 yr B.P, a 2-cm thick layer of *young* dense laminated tufa formed between 1159 and 1205 m. The laminated tufa is composed of low-magnesium calcite, indicating precipitation from a relatively fresh-water lake. During this time, *young* thinolitic and *young* branching tufas were eroded from the faces of Marble Bluff and Anaho Island between 1207 and ~1225 m (Benson et al., 1992). Dates on rock varnish coating boulders at an elevation of 1220 m on Anaho Island indicate that the lake occupied this elevation sometime between 10,850 and 9600 yr B.P. (Benson et al., 1992). The lake-level maximum that occurred at this time was coeval with the Younger Dryas Stade (Mangerud et al., 1974).

4.4. 9000–0 yr B.P.

A gap in tufa deposition exists between ~9000 and ~5000 yr B.P. For at least part of this time, Pyramid Lake may have been below 1159 m. Encrusting tufas and beachrock (Table 2) formed below 1183 m (the former elevation of Mud Lake Slough sill, see discussion in Benson, 1994). between 5080±60 and 1350±70 yr B.P. The relative thinness (<1.5-cm thick) of aragonitic encrusting tufas found between 1183 and 1159 m indicates the possibility that lake level remained below this depth interval during much of the late Holocene.

5. Change in effective wetness between 30,000 and 0 yr B.P.

Changes in effective wetness (Table 5), necessary to achieve spill from or to various Lahontan subbasins, were calculated using Eq. 1 and data listed in Table 6. It is impossible to associate a unique value of ΔW_{eff} with lake level in the Pyramid Lake subbasin between 1207 and 1308 m because of the possibility of river diversion (Benson and Paillet, 1989).

Values of ΔW_{eff} (Table 5) achieved by Lake Lahontan are indicated in Fig. 10. At 23,000 yr

Table 6
Surface areas (km^2) of Lahontan subbasins for some elevations (m). Data taken from Benson and Mifflin (1986)

Elevation	Pyramid Lake subbasin	Winnemucca Lake subbasin	Smoke Creek–Black Rock Desert subbasin	Carson Desert subbasin	Honey Lake subbasin	Buena Vista subbasin	Walker Lake subbasin
1177	568	256	–	–	–	–	–
1207	680	337	2514	–	–	–	–
1222	721	365	3066	–	535	–	–
1225	728	370	3139	–	543	–	–
1265	836	436	5809	5580	1140	505	–
1308	1003	517	8407	6846	1606	710	781
1335	1126	569	9152	8325	1692	812	1100

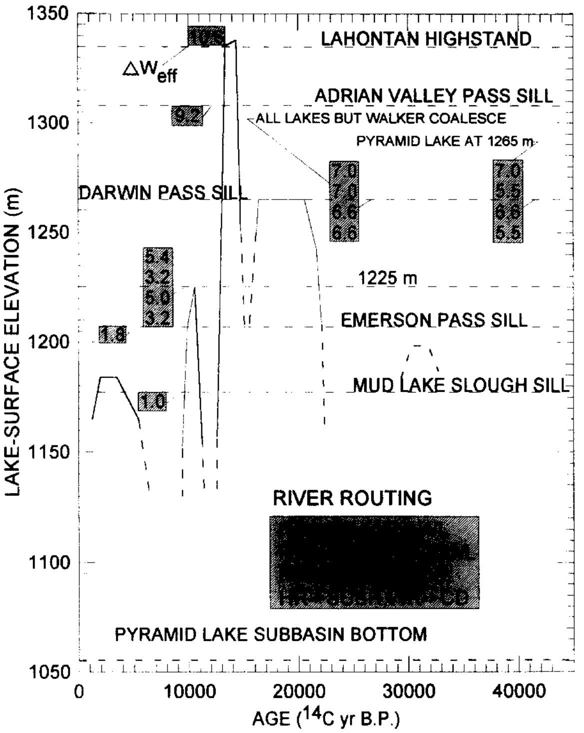

Fig. 10. Values of effective wetness (Δw_{eff}) associated with sill levels (spill points) and the 1225-m elevation in western Lahontan subbasins. When more than one value of Δw_{eff} is listed, the uppermost number was calculated for a situation in which the Humboldt River (*HR*) flows to the Carson Desert subbasin (*CD*) and the Walker River (*WR*) flows to Walker Lake (*WL*). The second number indicates a calculation made when HR flows to the Smoke Creek–Black Rock Desert subbasin (*BRD*) and WR flows to WL. The third number indicates a calculation made when HR flows to CD and WR flows to CD, and the fourth number indicates a calculation made when HR flows to BRD and WR flows to CD. When lakes in the western Lahontan subbasins reach 1265 m, either they spill into the Carson Desert (Δw_{eff}= 5.5) or they coalesce with Carson Lake (Δw_{eff}= 6.6–7.0) depending on the paths of the Lahontan rivers.

B.P., $\Delta W_{\mathrm{eff}} \leqslant 1.0$. When the western Lahontan subbasins first spilled to the Carson Desert subbasin, ΔW_{eff}= 5.5–7.0 (if the Humboldt River flowed to the Black Rock Desert). When the lakes in all subbasins excepting Walker Lake subbasin coalesced at 1265 m, ΔW_{eff} had a value of either 6.6 (Walker River flowed to Walker Lake) or 7.0 (Walker River flowed to the Carson Desert). The Lahontan highstand occurred when ΔW_{eff}= 10.6. If the Humboldt River diverted from the Black Rock Desert to the Carson Desert after the Lahontan highstand and the Walker River flowed to Walker Lake, ΔW_{eff} was of the same magnitude ~10,500 yr B.P. (ΔW_{eff}= 5.4) as it was when the lakes in the western Lahontan subbasins first reached 1265 m. During the late Holocene, $\Delta W_{\mathrm{eff}} \approx 1.0$.

6. The Lahontan lake-level record as an indicator of the position of the polar jet stream

Antevs (1938) was the first to link maximum levels of northern Great Basin lakes to the presence of a permanent ice sheet over North America, hypothesizing that the size of the ice sheet, combined with a permanent high-pressure area located over it, caused storm tracks to be pushed south of their present "normal" paths over northern Nevada and Utah. Renewed interest in this concept occurred in the mid 1980s when experiments using atmospheric general circulation models (Manabe and Broccoli, 1985; Kutzbach and Wright, 1985; Kutzbach and Guetter, 1986) indicated that glacial-age boundary conditions, including the size and shape of Laurentide Ice Sheet, were sufficient to produce the effect that Antevs had hypothesized. When the ice sheet was at a maximum (21,000–17,000 yr ago, Fig. 11), zonal flow aloft occurred across North America and the North Atlantic. The mean position of the southern branch of the jet stream lay south of the Lahontan basin in winter and over its northern edge in summer. Under these conditions of extensive cloudiness, decreased air temperature, and increased precipitation, lakes in the Lahontan basin increased in size (Hostetler and Benson, 1990).

With reductions in size and elevation of the ice sheet, the two branches of the jet stream recombined. Flow aloft became meridional and the paths of the winter and summer jet streams remained north of the Lahontan basin. Climate of the Lahontan basin became dry and warm and lake levels declined. During solar forced growth and decay of the Laurentide Ice Sheet, Lake Lahontan should have experienced two lake-level maxima corresponding to the pre- and post-maximum gla-

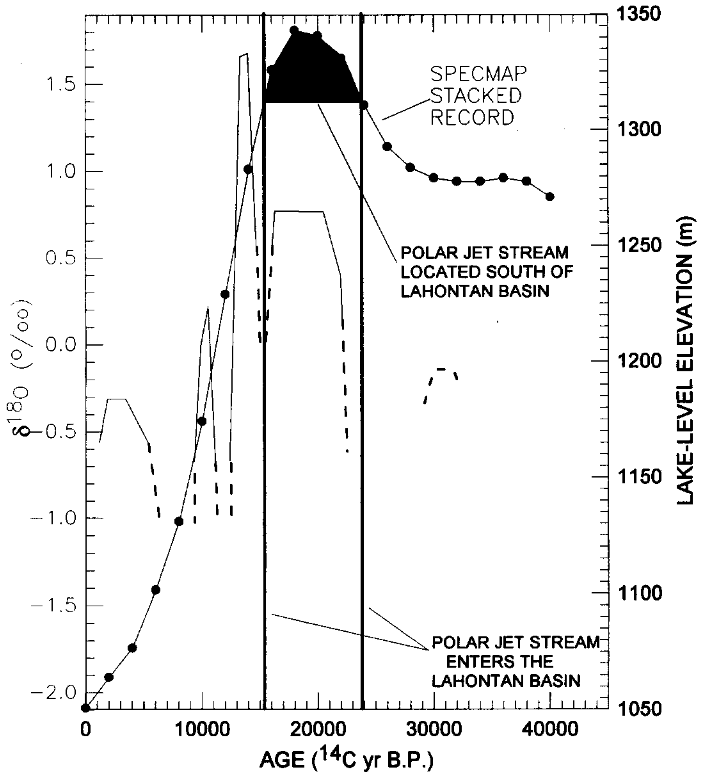

Fig. 11. A comparison of the SPECMAP stacked marine $\delta^{18}O$ record (Imbrie et al., 1984) with the Lahontan lake-level envelope. The marine $\delta^{18}O$ record is a proxy for the amount of ice stored in the world's glaciers. Increasing values of marine $\delta^{18}O$ indicate increasing amounts of stored ice. The major increases in lake level that occur at ~23,500 and 15,500 yr B.P. are associated with a $\delta^{18}O$ value of ~1.4. We believe that this particular value is indicative of an ice sheet whose size and shape is sufficient to force the polar jet stream over the Lahontan basin. When the core of the jet stream overlies the basin (Laurentide Ice Sheet is increasing in size), increases in cloudiness and rainfall and decreases in air temperature occur. When the core of the jet stream lies south of the basin (during maximum extent of Laurentide Ice Sheet), the basin is still cold and cloud covered, but much of the increased precipitation associated with the jet stream core falls south of the basin. When the core of the jet stream lies north of the basin (Laurentide Ice Sheet has retreated), the climate becomes less cloudy, warm, and arid.

cial passages of the jet stream core over the Lahontan basin. This concept is borne out by evidence that Lake Lahontan abruptly increased in size starting ~23,500 and ~15,500 yr B.P. (Fig. 11) when the globally integrated $\delta^{18}O$ value of seawater was 1.4‰ (Imbrie et al., 1984). The assumption made here is that the globally integrated $\delta^{18}O$ value of seawater is a reasonable proxy, not only for world-wide ice volume, but also for volume of the Laurentide Ice Sheet.

The abruptness of the two lake-level rises is hypothesized to reflect the encounter of precipitation maxima, located near the jet-stream core (Starrett, 1949), with the Lahontan basin. Differences in elevations of the two lake-level maxima were due to differences in the residence times of the jet stream over the Lahontan basin and differences in the initial sizes of the lakes. When the jet stream core passed over the lake ~23,500 yr ago, the lake was small; however, when the jet stream moved northward over the lake in response to reduction in size of the Laurentide Ice Sheet ~15,500 yr ago, the lake was already relatively large.

Some of the major features in the Lahontan lake-level envelope cannot be explained by solar-forced changes in the size of the Laurentide Ice Sheet; e.g., the lake-level oscillation between 11,000 and 10,000 yr B.P. and the lake-level minima at ~15,500 yr B.P. An explanation of these phenomena is beyond the scope of this paper.

7. A comparison of the Lake Lahontan and Lake Bonneville lake-level records

Lake Bonneville's drainage lay to the west of and on about the same latitude as Lake Lahontan's drainage. We would, therefore, expect that the hydrologic balances of Lake Bonneville and Lake Lahontan would covary with movement of the polar jet stream. A lake-level envelope for the Bonneville basin between 32,000 and 0 yr B.P. (Fig. 12) was constructed using data presented in Oviatt et al. (1992). Values of ΔW_{eff} calculated from the hypsographic data of Currey et al. (1984) have also been affixed to the lake-level envelope (Fig. 12). Lake Bonneville was at low levels

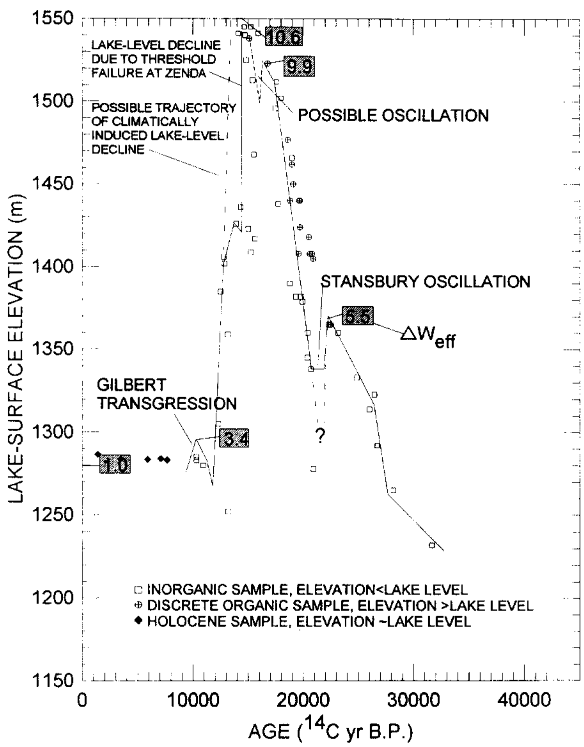

Fig. 12. Lake Bonneville record for the past 30,000 yr. Values of effective wetness (Δw_{eff}) are indicated in shaded squares. Data for this figure were taken from Oviatt et al. (1992).

between 32,000 and 27,000 yr B.P. After 27,000 yr B.P. the lake rose reaching its highest level by ~15,000 yr B.P. Two oscillations (lake-level minima) occurred at ~21,000 and ~16,000 yr B.P. The minimum elevation of the Stansbury oscillation remains somewhat conjectural (Oviatt et al., 1990; Thompson et al., 1990). The elevation (~1340 m) of the solid line at 21,000 yr B.P. is based on the lowest occurrence of a shallow-water sand associated with the oscillation (Oviatt et al., 1990).

The magnitude and timing of the 16,000 yr B.P. oscillation (Keg Mountain oscillation) also remains in doubt. The Keg Mountain oscillation was originally hypothesized to have consisted of a 45-m decline in lake level, with the lowest point of the oscillation being achieved immediately prior to the eruption of the Pahvant Butte ash (Currey and Oviatt, 1985). A recent reevaluation of the evidence for the Keg Mountain oscillation indicates that a transgressive phase oscillation of lesser magnitude could also explain the stratigraphic sequence found at its type locality (Oviatt et al., 1994). Existing evidence indicates that the lower limit of the Keg Mountain oscillation was ~1500 m (Oviatt et al., 1994).

Lake Bonneville receded from its highest shoreline as the result of the catastrophic downcutting of the basin margin ~14,500 yr B.P. For this reason, we do not know what elevation Lake Bonneville would have achieved after 14,500 yr B.P. or when it would have fallen in response to the northward movement of the polar jet stream. A dashed line indicating the possible timing of the climatic induced fall of Lake Bonneville is shown on Fig. 12. At ~12,000 yr B.P., Great Salt Lake was at very low levels and a subsequent transgression of Great Salt Lake to the Gilbert shoreline culminated between 10,900 and 10,300 yr B.P. (Currey, 1990).

The Lahontan and Bonneville chronologies compare reasonably well in terms of the timing of lake-level decline and fall and in terms of effective wetness between ~21,000 and 9000 yr B.P. (Figs. 10 and 12). Lake Bonneville appears to have risen more rapidly between 21,000 and 16,500 yr B.P. than Lake Lahontan, achieving a ΔW_{eff} of 9.9. The ΔW_{eff} of the Lahontan system was between

5.5 and 7.0 at 16,500 yr B.P. (Fig. 10). Both lake systems recorded a decrease in level of uncertain magnitude at ~16,000 yr B.P. Given the uncertainty in the timing of the climatically induced fall of Lake Bonneville, both lakes can be hypothesized to have begun receding at ~13,000 yr B.P. Both lake systems experienced low levels at ~12,000 yr B.P. and both lakes also experienced a final lake-level transgression that resulted in higher levels at ~10,500 yr B.P. Age and elevation control for both lake systems prior to 22,000 yr B.P. is too inaccurate and too discontinuous to permit a meaningful comparison of the two systems. However, the covariance in lake-level variation after 22,000 yr B.P. suggests that both systems were responding nearly synchronously with variation in the positon of the polar jet stream.

8. Summary and conclusions

Most tufas in the Pyramid Lake subbasin, including the large mound formations that border the existing lake, were deposited within the last 35,000 yr. Tufa deposition in the Holocene was discontinuous in time and small in magnitude. Older (>21,000 yr B.P.) tufas (*old* tubular and *old* branching tufas) probably were deposited in association with ground-water discharge; thus, their ^{14}C ages should be considered maximum estimates of their time of formation.

The Lahontan lake-level envelope developed from tufa elevations and ^{14}C ages indicates the following: (1) for at least part of the time between ~27,500 and 23,500 yr B.P., Lake Lahontan was at a low elevation (~1165 m); (2) by ~21,000 yr B.P., Lake Lahontan had reached the elevation of Darwin Pass Sill and remained near this elevation (1265 m) for the next 5000 yr; (3) Lake Lahontan fell below an elevation of 1252 m by ~15,500 yr B.P.; (4) by 14,500 yr B.P., lakes in all Lahontan subbasins had reached 1308 m and had coalesced; (5) by 13,800 yr B.P., Lake Lahontan achieved its last highstand (>1330 m), and at 13,600 yr B.P., it began to recede; (6) by 12,400 yr B.P., Lahontan had receded to an elevation of ~1160 m; (7) between 12,000 and 11,000 yr B.P., Lake Lahontan probably remained below 1160 m; (8) between 11,000 and 9000 yr B.P., Lake Lahontan experienced a profound oscillation in level, rising to an elevation of ~1225 m by 10,500 yr B.P.; (9) between ~9000 and ~5000 yr B.P., no lake level data exist; and (10) between 5000 and 1400 yr B.P., lake level remained at or below 1183 m, the early Holocene elevation of the spill point to the Winnemucca Lake subbasin.

Much of the carbonate in the mound complexes was deposited between 30,000 and 12,000 yr B.P. This time interval is essentially synchronous with the last major lake cycle in the Lahontan basin, indicating that ground- and surface-water discharge varied together during the last last cycle.

Acknowledgments

My appreciation is expressed to those who reviewed earlier versions of this manuscript including James Bischoff, Ted McConnaughey, and Robert Rye of the U.S. Geological Survey. I also thank the Pyramid Lake Paiute Tribal Council for access to the Pyramid Lake Reservation. Charles "Jack" Oviatt of Kansas State University and Kerry Kelts of the University of Minnesota provided thoughtful reviews of the final manuscript.

This work was performed in part under the auspices of the US Department of Energy by Lawrence Livermore National Laboratory under contract W-7405-ENG-48.

References

Antevs, E., 1938. Postpluvial climatic variations in the southwest. Bull. Am. Meteorol. Soc., 19: 190–193.

Benson, L.V., 1978. Fluctuation in the level of pluvial Lake Lahontan during the last 40,000 years. Quat. Res., 9: 300–318.

Benson, L.V., 1993. Factors affecting ^{14}C ages of lacustrine carbonates: timing and duration of the last highstand lake in the Lahontan Basin. Quat. Res., 39: 163–174.

Benson, L.V., 1994a. Carbonate deposition, Pyramid Lake Subbasin, Nevada: 1. Sequence of formation and elevational distribution of carbonate deposits (Tufas). Palaeogeogr. Palaeoclimatol. Palaeoecol., 109: 55–87.

Benson, L.V. and Mifflin, M.D., 1986. Reconnaissance bathymetry of basins occupied by Pleistocene Lake Lahontan, Nevada and California. U.S. Geol. Surv. Water-Resour. Invest. Rep., 85-4262, 14 pp.

Benson, L.V. and Paillet, F.L., 1989. The use of total lake-surface area as an indicator of climatic change: examples from the Lahontan basin. Quat. Res., 32: 262–275.

Benson, L.V. and Thompson, R.S., 1987. Lake-level variation in the Lahontan Basin for the past 50,000 years. Quat. Res., 28: 69–85.

Benson, L.V., Currey, D., Lao, Y. and Hostetler, S., 1992. Lake-size variations in the Lahontan and Bonneville basins between 13,000 and 9000 ^{14}C yr B.P. Palaeogr., Palaeoclimatol., Palaeoecol., 95: 19–32.

Currey, D.R., 1990. Quaternary paleolakes in the evolution of semidesert basins, with special emphasis on Lake Bonneville and the Great Basin, U.S.A. Palaeogeogr. Palaeoclimatol. Palaecol., 76: 189–214.

Berger, G.W., 1991. The Use of Glass for Dating Volcanic Ash by Thermoluminescence. J. Geophys. Res., 96: 19,705–19,720.

Bischoff, J.L., Fitzpatrick, J.A. and Rosenbauer, R.J., 1993. The solubility and stabilization of ikaite ($CaCO_3 \cdot 6H_2O$) from 0° to 25°C: Environmental and paleoclimatic implications for thinolite tufa. J. Geol., 101: 21–33.

Broecker, W.S. and Kaufman, A., 1965. Radiocarbon chronology of Lake Lahontan and Lake Bonneville II, Great Basin. Geol. Soc. Am. Bull., 76: 537–566.

Broecker, W.S. and Walton, A.F., 1959. The geochemistry of ^{14}C in freshwater systems. Geochim. Cosmochim. Acta, 16: 15–38.

Currey, D.R. and Oviatt, C.G., 1985. Durations, average rates, and probable causes of Lake Bonneville expansions, 32,000 to 10,000 years ago. In: P.A. Kay and H.F. Diaz (Editors), Problems of and Prospects for Predicting Great Salt Lake Levels. Cent. Public Affairs Adm., Univ. Utah, Salt Lake City, pp. 9–24.

Currey, D.R., Atwood, G. and Mabey, D.R., 1984. Major levels of Great Salt Lake and Lake Bonneville. Utah Geol. Min. Surv. Map 73.

Dansie, A., Davis, J.O. and Stafford Jr., T.W., 1990. The Wizards beach recession: Farmdalian (25,500 year BP) vertebrate fossils co-occur with early Holocene artifacts. In: J.A. Willig, C.M. Aikens and J.L. Fagan (Editors), Early Human Occupation in Far Western North America: the Clovis–Archaic Interface. Nev. State Mus. Anthropol. Pap., 21: 153–200.

Davis, J.O., 1978. Quaternary tephrochronology of the Lake Lahontan area, Nevada and California. Nev. Archeol. Surv. Pap., 7, 123 pp.

Davis, J.O., 1982. Bits and pieces; The last 35,000 years in the Lahontan area. In: D.B. Madsen and J.F. O'Connell (Editors), Man and Environment in the Great Basin. Soc. Am. Archeol. Pap., 2: 53–75.

De Deckker, P. and Last, W.M., 1988. Modern dolomite deposition in continental, saline lakes, western Victoria, Australia. Geology, 16: 29–32.

Erickson III, D.J., 1993. A stability dependent theory for air–sea gas exchange. J. Geophys. Res., 98: 8471–8488.

Hostetler, S.W. and Benson, L.V., 1990. Paleoclimatic implications of the high stand of Lake Lahontan derived from models of evaporation and lake level. Clim. Dyn., 4: 207–217.

Imbrie, J., Hays, J.D., Martinson, D.G., McIntyre, A., Mix, A.C., Morley, J.J., Pisias, N.G., Prell, W.L. and Shackleton, N.J., 1984. The orbital theory of Pleistocene climate: support from a revised chronology of the marine $\delta^{18}O$ record. In: A. Berger, J. Imbrie, J. Hays, G. Kukla and B. Saltzman (Editors), Milankovitch and Climate, Part 1 (NATO ASI Ser. C, 126). Reidel, Dordrecht, pp. 269–305.

King, G.Q., 1978. The late Quaternary history of Adrian Valley, Lyon County, Nevada. Thesis. Univ. Utah, Salt Lake City, 88 pp.

Kutzbach, J.E. and Guetter, P.J., 1986. The influence of changing orbital parameters and surface boundary conditions on climate simulations for the past 18000 years. J. Atmos. Sci., 43: 1726–1759.

Kutzbach, J.E. and Wright Jr., H.E., 1985. Simulation of the climate of 18,000 yr B.P.: Results for the North American/North Atlantic/European Sector and comparison with the geologic record of North America. Quat. Sci. Rev., 4: 147–187.

Lao, Y. and Benson, L.V., 1988. Uranium-series age estimates and paleoclimatic significance of Pleistocene tufas from the Lahontan basin, California and Nevada. Quat. Res., 30: 165–176.

Manabe, S. and Broccoli, A.J., 1985. The influence of continental ice sheets on the climate of an ice age. J. Geophys. Res., 90: 2167–2190.

Mangerud, J., Andersen, S.T., Berglund, B.E. and Donner, J.J., 1974. Quaternary stratigraphy of Norden, a proposal for terminology and classification. Boreas, 3: 109–128.

Oviatt, C.G., Currey, D.R. and Miller, D.M., 1990. Age and paleoclimatic significance of the Stansbury oscillation of Lake Bonneville, northeastern Great Basin. Quat. Res., 33: 291–305.

Oviatt, C.G., Currey, D.R. and Sack, D., 1992. Radiocarbon chronology of Lake Bonneville, eastern Great Basin, USA. Palaeogeogr. Palaeoclimatol. Palaeoecol., 99: 225–241.

Oviatt, C.G., Sack, D. and Felger, T.J., 1994. Quaternary geologic map of the Old River Bed and vicinity, Millary, Juab, and Tooele Counties, Utah. Utah Geol. Map, 16, 1:62,500, 24 pp.

Pauly, H., 1963. Ikaite, a new mineral from Greenland. Arctic, 16: 263–264.

Shearman, D.J., McGugan, A., Stein, C. and Smith, A.J., 1989. Ikaite, $CaCO_3.6H_2O$, precursor of the thinolites in the Quaternary tufas, and tufa mounds of the Lahontan and Mono Lake Basins, western United States. Geol. Soc. Am. Bull., 101: 913–917.

Stafford Jr., T.W., Hare, P.E., Currie, L., Jull, A.J.T. and Donahue, D.J., 1991. Accelerator radiocarbon dating at the molecular level. J. Archaeol. Sci., 18: 35–72.

Starrett, L.G., 1949. The relation of precipitation patterns in North America to certain types of jet streams at the 300-millibar level. J. Meteorol., 6: 347–352.

Stuiver, M. and Polach, H.A., 1977. Discussion reporting of ^{14}C data. Radiocarbarbon, 19: 355–363.

Thompson, R.S., Benson, L.V. and Hattori, E.M., 1986. A revised chronology for the last Pleistocene lake cycle in the central Lahontan basin. Quat. Res., 25: 1–9.

Thompson, R.S., Toolin, L.J., Forester, R.M. and Spencer, R.J., 1990. Accelerator-mass spectrometer (AMS) radiocarbon dating of Pleistocene lake sediments in the Great Basin. Palaeogeogr. Palaeoclimatol. Palaeoeccol., 78: 301–313.

U.S. Geol. Surv., 1984–1993. Water resources data for Nevada. U.S. Geol. Surv. Water-Data Rep. Ser., Ann. Vol.

Wright Jr., H.E., 1989. The amphi-Atlantic distribution of the Younger Dryas paleoclimatic oscillation. Quat. Sci. Rev., 8: 295–306.

York, D., 1979. Least squares fitting of a straight line with correlated errors. Earth Planet. Sci. Lett., 5: 320–324.